Cell Culture and Transfection. Huh-7 human HCC cells, U-2 OS human osteosarcoma cells, 293T human embryonic kidney cells, mouse lymph node cells, and P3X63Ag8U.1 mouse myeloma cells were cultured in Dulbecco's modified Eagle's medium (Gibco BRL Life Technologies, NY) supplemented with 10% fetal bovine serum as described.[16] To assess viable cell numbers, we used the Dojindo Cell Counting Kit-8 (CCK8 kit, Dojindo Laboratories, Kumamoto, Japan) according to the manufacturer's instructions.

The 293T, Huh-7, and U-2 OS cells were transfected with plasmid DNA by using the calcium phosphate method or FuGENE 6 Transfection Reagent (Roche Diagnostics, Mannheim, Germany) as described.[16] Short interfering RNA (siRNA) were transfected at a final concentration of 25 nM by using siPORT NeoFX Transfection Agent (Ambion, Austin, TX) following the manufacturer's instructions. Twenty-four hours after transfection, the medium was replaced with fresh medium containing fetal bovine serum, and the culture was continued for another 24 or 48 hours. Then, the cells were harvested for analysis. All transfection assays were repeated at least 3 times.

Plasmids and siRNA. Human wild-type gankyrin cDNAs, full coding sequence and deletion mutants, were cloned into the mammalian expression vector pMKIT-NEO and expressed as hemagglutinin (HA)-tagged proteins (Fig. 1A). Full-length gankyrin was expressed without a tag as well. To obtain recombinant human gankyrin protein, the full-length cDNA was cloned into an expression vector derived from pET28 (Novagen, EMD Biosciences Inc., San Diego, CA) and expressed as hexahistidine-tagged protein.

To down-regulate gene expression, Silencer Predesigned siRNAs for gankyrin (Ambion) and Stealth Select iRNA: for IGFBP-5 (Invitrogen, Tokyo, Japan), were used together with respective control RNAs.

Antibodies. To obtain monoclonal antibodies against human gankyrin, recombinant (His)6-gankyrin protein was used as an immunogen. It was dissolved in phosphate-buffered saline (1 mg/mL) and emulsified with an equal volume of Freund's complete adjuvant (Difco, Becton-Dickinson, Franklin Lakes, NJ). Two female BALB/c mice were injected with the emulsion (50 μL/mouse) in the footpad. Two weeks after immunization, the inguinal lymph node cells (4×10^7 cells) were fused with P3X63Ag8U.1 myeloma cells (1×10^7) using polyethylene glycol 1500 (Roche Diagnostics). Fused cells were cultured in 96-well plates at 2×10^5 cell/well. The supernatants were assayed for the anti-gankyrin antibody titer by an enzyme-linked immunosorbent assay using recombinant His-tagged, glutathione-S-transferase (GST)-tagged, and nontagged gankyrin proteins. Selected relevant hybridomas were cloned by the limiting dilution method, and the isotypes of secreted monoclonal antibodies were determined by the IsoStrip kit (Roche Diagnostics) following the manufacturer's instructions. Finally, an IgG2b kappa monoclonal antibody that showed the highest affinity for gankyrin was obtained and named 3A6C2.

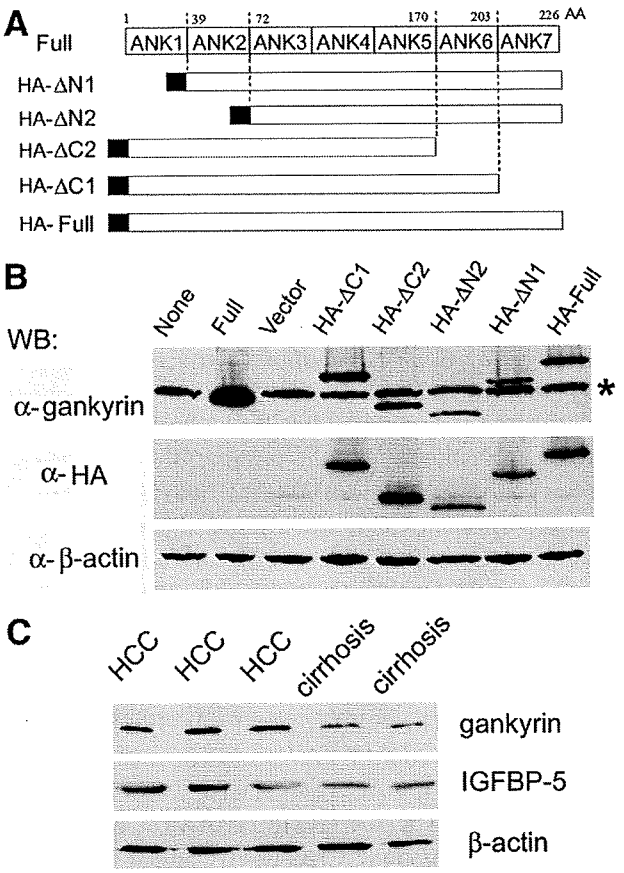

Fig. 1. Recognition of gankyrin protein by the monoclonal antibody. (A) Structures of wild-type gankyrin (Full) and its deletion mutants. Numbers on top, N- and C-terminal amino-acid residues. ANK, ankyrin repeat. Black bars, HA tags. (B) Specificity of the antibody. 293T cells were transfected with plasmids expressing the indicated proteins. Cell lysates were analyzed by western blotting (WB) using the anti-gankyrin monoclonal antibody (3A6C2), anti-HA antibody, and anti-β-actin antibody. *Mobility of the endogenous gankyrin. Representative results of 3 repeated experiments are shown. (C) Detection of gankyrin protein in tissues. Lysates were made from hepatocellular carcinoma (HCC, n = 3) and cirrhotic liver tissues (n = 2), and analyzed by WB using antibodies for indicated proteins. HA, hemagglutinin.

For western blot analysis, mouse monoclonal anti-gankyrin antibody (3A6C2), goat polyclonal anti–IGFBP-5 antibody (R&D Systems Inc., Minneapolis, MN), mouse monoclonal anti-HA antibody (12CA5, Roche Diagnostics), and mouse monoclonal anti–β-actin antibody (Chemicon International, Temecula, CA) were

used. Horseradish peroxidase–conjugated secondary antibodies against mouse or goat immunoglobulins were obtained from DAKO (Kyoto, Japan).

For immunohistochemistry, mouse monoclonal anti-gankyrin (3A6C2), anti-MDM2 (Ab-4, Oncogene research products, Boston, MA), and anti-p53 (DO-7, DAKO) antibodies, rabbit polyclonal anti-IGFBP-5 antibody (GroPep, Thebarton, Australia), and horseradish peroxidase–conjugated secondary antibodies against mouse or rabbit immunoglobulins (DAKO) were used.

Analysis of Gene Expression. Extraction of RNA, preparation of cell and tissue lysates, and western blot analysis were performed as described.[9] Real-time reverse transcription polymerase chain reaction (RT-PCR) analysis was performed using ABI PRISM 7900 (Applied Biosystems, Foster City, CA) and a 1-step QuantiTect RT-PCR Kit (Qiagen, Cowley, UK) according to the manufacturer's instructions. PCR conditions were 50°C for 30 minutes and 95°C for 15 minutes, followed by 45 cycles of 95°C for 15 seconds, 55°C for 30 seconds, and 72°C for 45 seconds. Specific PCR amplification products were detected by SYBR Green. Transcripts of β-actin were quantified as control. Primer sequences used were as follows: IGFBP-5, AAGAAGCTGACCCAGTCCAA and GAATCCTTTGCGGTCACAAT; gankyrin, GCAACTTGGAGTGCCAGTGAA and TCACTTGAGCACCTTTTCCCA; β-actin, CTACGTCGCCCTGGACTTCGAGC and GATGGAGCCGCCGATCCACACGG.

The immunohistochemical staining was performed on 4-μm-thick paraffin sections of tissues fixed in buffered formalin. The sections were pretreated with 10 mM citrate buffer (pH 6.1) in a microwave oven for 5 minutes. Endogenous peroxidase activity was blocked with 0.3 % H_2O_2 for 10 minutes. The sections were incubated with 10% fetal bovine serum for 30 minutes to reduce nonspecific binding, followed by incubation with the primary antibody at 4°C overnight. They were subsequently incubated with horseradish peroxidase–conjugated anti-mouse or rabbit immunoglobulin antibody for 30 minutes. The enzymatic reaction was developed in a freshly prepared solution of 3,3′-diaminobenzidine tetrahydrochloride using DAKO Liquid DAB Substrate-Chromogen Solution for 10 minutes at room temperature. The sections were then counterstained with hematoxylin. The staining pattern, the distribution of the immunostaining in each tissue, and the intensity of the staining were studied in detail. Negative controls were conducted by substituting normal sera of each animal for the primary antibodies. When immunoreactivities were heterogenously observed, cases with moderate or strong staining of nucleus or cytoplasm in more than 5% of the cells were considered positive. To analyze the correlation of the expression levels of gankyrin and IGFBP-5, the staining intensity was expressed as 0 (negative), 1+ (weakly positive), 2+ (moderately positive), or 3+ (strongly positive). In each case the immunoreactivity was determined in 5 random high-powered fields and the count was done independently by 2 observers.

Statistical Analysis. Categorical variables were compared using Fisher's exact test. Paired comparison of continuous data was performed using the Wilcoxon signed ranks test. To assess whether the 2 variables covary, Spearman's rank correlation coefficient was determined. Cumulative survival curves were calculated by the Kaplan-Meier method and analyzed by the log-rank test. All statistical analyses were performed using the JMP statistical software package (SAS Institute Inc., Cary, NC). A P value less than 0.05 was considered statistically significant.

Results

Clinicopathological Profiles. Forty-three patients with HCC were recruited in this study, including 27 men and 16 women, with ages ranging from 25 to 78 (median 65) years old. Clinicopathological profiles of the patients and their HCCs are shown in Table 1. Antibody to hepatitis C virus was found in sera of 72% of the patients, and hepatitis B virus surface antigen was positive in 21%.

According to the TNM staging, 60% were stage I to II and 40% were stage III to IV. In noncancerous portions of the resected livers, cirrhosis and chronic hepatitis[18] were found in 68% and 30%, respectively, of the specimens, whereas only 1 (2%) was of normal histology. Fibrocapsular formation surrounding HCC was observed in 84% and capsular invasion by HCC cells in 33%. Portal vein involvement and satellite nodules suggesting intrahepatic metastasis were found in 21% and 37%, respectively.

Detection of Gankyrin with the Monoclonal Anti-gankyrin Antibody. To determine the specificity of the monoclonal anti-gankyrin antibody 3A6C2, we expressed wild-type full-length or truncated gankyrin (Fig. 1A) in 293T cells. The antibody detected all mutants of gankyrin, suggesting that the epitope exists within the third and fifth ankyrin-repeat region (Fig. 1B). The antibody recognized the endogenous gankyrin as well, and no major cross-reacting band was observed.

Because gankyrin mRNA is known to be overexpressed in most HCCs,[9] we analyzed the levels of gankyrin protein in HCCs and surrounding noncancerous liver tissues using the 3A6C2 antibody. The protein level of gankyrin was higher in HCC tissues than in noncancerous tissues

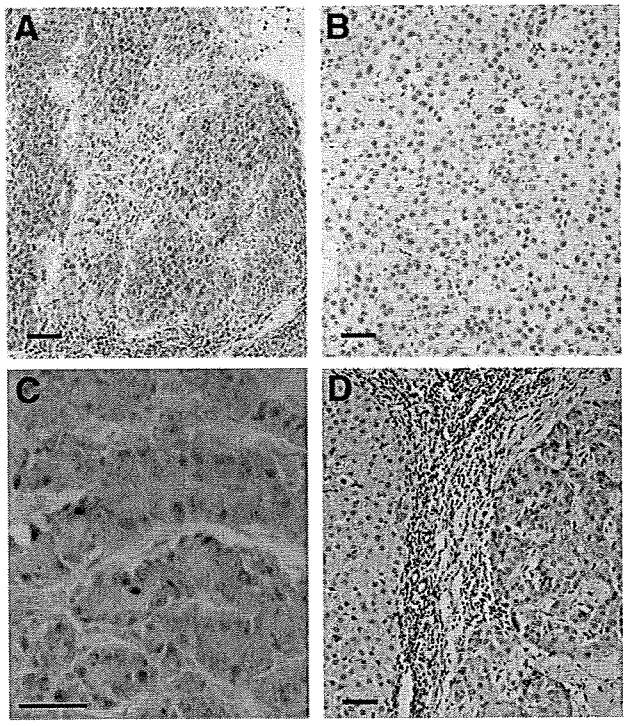

Fig. 2. Immunohistochemical detection of gankyrin in hepatocellular carcinoma (HCC). HCC sections were stained with mouse monoclonal anti-gankyrin antibody, and counterstained with hematoxylin. Positive immunostaining appears brown. (A) Positive staining for gankyrin in the cytoplasm of most HCC cells. (B) Barely detectable gankyrin signal in some HCC cells. (C) Presence of gankyrin in the nucleus of some HCC cells. (D) Stronger staining for gankyrin in HCC cells (right) than the neighboring cirrhotic hepatocytes (left). Bar, 50 μm.

(Fig. 1C). The mobilities of the gankyrin band were not different among samples.

Immunohistochemical Analysis of Gankyrin Expression. We next examined the expression of gankyrin protein in HCC and noncancerous liver tissues by immunohistochemistry. The gankyrin signal was observed mainly in the cytoplasm and occasionally in the nucleus of HCC cells (Fig. 2A-C). Although at lower levels compared with those in HCCs, weak but reproducible gankyrin signals were observed in the cytoplasm of the hepatocytes in the noncancerous tissues (Fig. 2D). Expression of gankyrin was not detected in the bile duct cells, blood endothelial cells, or other nonparenchymal cells in the liver tissues. Of 43 HCCs examined, the cytoplasm was stained positively for gankyrin in 27 (63%), and 9 of them (21%) were also positive for nuclear staining. Of 32 noncancerous liver tissues available, gankyrin was positive in 17 (53%).

As shown in Table 2, we analyzed an association between gankyrin protein expression and clinicopathological findings. No significant association between gankyrin expression in HCC cells and sex, age, tumor size, fibrotic change in noncancerous liver tissues, differentiation of the tumor cells, or hepatitis B or C virus infection was observed. Positive cytoplasmic staining for gankyrin of HCC cells was significantly associated with low TNM stage (stage I or II; $P = 0.004$), no capsular invasion ($P = 0.018$), no portal venous invasion ($P = 0.008$), and no intrahepatic metastasis ($P = 0.012$) of HCC. In noncancerous liver tissues, positive gankyrin staining of hepatocytes was associated with the cytoplasmic gankyrin positivity of HCC cells of the same patient ($P = 0.021$, Table 3), but not with the parameters examined except for the serum alpha-fetoprotein level ($P = 0.015$, Table 2).

Because expression of gankyrin affects the degradation of p53 and MDM2,[16] we examined the expression of p53 and MDM2 as well as gankyrin in HCCs. By immunohistochemistry, nuclear expression of p53 and MDM2 were detected in 30% and 23%, respectively, of 43 HCCs (Fig. 3, Table 3). Positive staining for gankyrin was not associated with the staining for p53 nor MDM2 in HCC cells.

Up-regulation of IGFBP-5 Expression by Gankyrin in HCCs. Preliminary microarray analysis of the cDNA libraries prepared from U-2 OS cells and Huh-7 cells overexpressing gankyrin suggested that IGFBP-5 mRNA was up-regulated by gankyrin (A. Umemura and J. Fujita, unpublished data). Real-time RT-PCR analysis con-

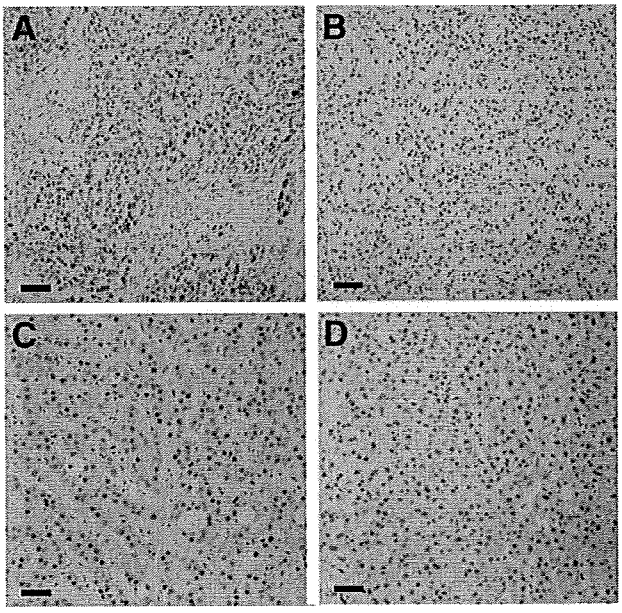

Fig. 3. Immunohistochemical detection of p53 and MDM2 in hepatocellular carcinoma (HCC). HCC sections were stained with antibodies specific to p53 (A and B) or MDM2 (C and D), and counterstained with hematoxylin. Positive immunostaining appears brown. (A) Positive staining for p53 in the nucleus of most HCC cells. (B) Negative p53 in HCC cells. (C) Positive staining for MDM2 in the nucleus of most HCC cells. (D) Negative MDM2 in HCC cells. Bar, 50 μm.

Table 2. Gankyrin Expression and Clinicopathological Characteristics

	Gankyrin Expression in the Cytoplasm of					
	HCC			Noncancerous Liver		
	Negative (n = 16)	Positive (n = 27)	*P* value	Negative (n = 15)	Positive (n = 17)	*P* value
Sex distribution						
Male	12	15	0.328	10	11	1.000
Female	4	12		5	6	
Median age (years)	64	65	0.696	63	62	0.649
Virus marker			NS			NS
HBV(+)/HCV(−)	3	3		2	2	
HBV(−)/HCV(+)	10	18		11	11	
HBV(+)/HCV(+)	1	2		2	0	
HBV(−)/HCV(−)	2	4		0	4	
Median AFP (ng/mL)	63.0	95.0	0.890	25.0	199.0	0.015
Median tumor size (cm)	4.5	4.0	0.098	4.5	4.0	0.372
Liver cirrhosis (+)	9	20	0.316	9	13	0.450
TNM stage						
I and II	5	21	0.004	8	12	0.467
III and IV	11	6		7	5	
Histological differentiation						
Well	5	7	0.737	6	3	0.243
Moderate and poor	11	20		9	14	
Capsular formation (+)	15	21	0.229	12	13	1.000
Capsular invasion (+)	9	5	0.018	4	6	0.712
Portal venous invasion (+)	7	2	0.008	4	3	0.678
Intrahepatic metastasis (+)	10	6	0.012	6	5	0.712
Gankyrin nuclear expression						
Yes	0	9	0.016	2	5	0.403
No	16	18		13	12	

Abbreviations: HCV, anti-hepatitis C virus antibody; HBV, hepatitis B surface antigen; (+), positive or present; (−), negative or absent; AFP, serum alpha-fetoprotein; NS, not significant between any groups or combinations thereof.

firmed that overexpression of gankyrin increased the IGFBP-5 mRNA levels 5.2-fold and 1.7-fold (mean, n = 3 each) in U-2 OS and Huh-7 cells, respectively, and western blot analysis demonstrated that the protein levels were increased as well (Fig. 4A). Conversely, when gankyrin expression was suppressed by siRNA, IGFBP-5 expression was down-regulated (Fig. 4B). In 2 of 3 HCC tissues overexpressing gankyrin, the levels of IGFBP-5 protein were higher compared with those in noncancerous tissues (Fig. 1C). To identify a role that IGFBP-5 might play in HCC cells, we next suppressed IGFBP-5 expression by siRNA. No apoptosis was induced, but viable cell numbers were decreased in Huh-7 as well as U-2 OS cells (Fig. 4C,D, and data not shown), suggesting a growth-promoting effect of IGFBP-5.

The expression of IGFBP-5 was further examined immunohistochemically in 43 HCC and 32 noncancerous liver tissues (Fig. 5, Table 3). In 42% of HCCs, IGFBP-5 was positively stained in the cytoplasm of HCC cells (Fig. 5A). IGFBP-5 was also detected, although at lower levels, in the cytoplasm of hepatocytes in 28% of the noncancerous tissues (Fig. 5B-D), but not in bile duct cells, blood endothelial cells, or other nonparenchymal cells.

Specific cytoplasmic staining for IGFBP-5 in HCC cells was associated with low TNM stage (stage I or II; $P = 0.013$), no portal venous invasion ($P = 0.006$), low serum alpha-fetoprotein value ($P = 0.031$), and small tumor size ($P = 0.009$). No association with capsular invasion or intrahepatic metastasis was observed. There was a significant association between positivities for IGFBP-5 and

Table 3. Gankyrin Expression and Molecular Histological Markers

	Gankyrin Expression in HCC		
	Negative	Positive	*P* value
Gankyrin expression in non-HCC			
Negative (n = 15)	8	7	0.021
Positive (n = 17)	2	15	
p53 expression in HCC			
Negative (n = 30)	11	19	1.000
Positive (n = 13)	5	8	
MDM2 expression in HCC			
Negative (n = 33)	14	19	0.276
Positive (n = 10)	2	8	
IGFBP-5 expression in HCC			
Negative (n = 25)	13	12	0.026
Positive (n = 18)	3	15	
IGFBP-5 expression in non-HCC			
Negative (n = 23)	14	9	0.011
Positive (n = 9)	1	8	

Abbreviations: HCC, hepatocellular carcinoma; non-HCC, noncancerous portion of the resected liver; IGFBP-5, insulin-like growth factor-binding protein 5.

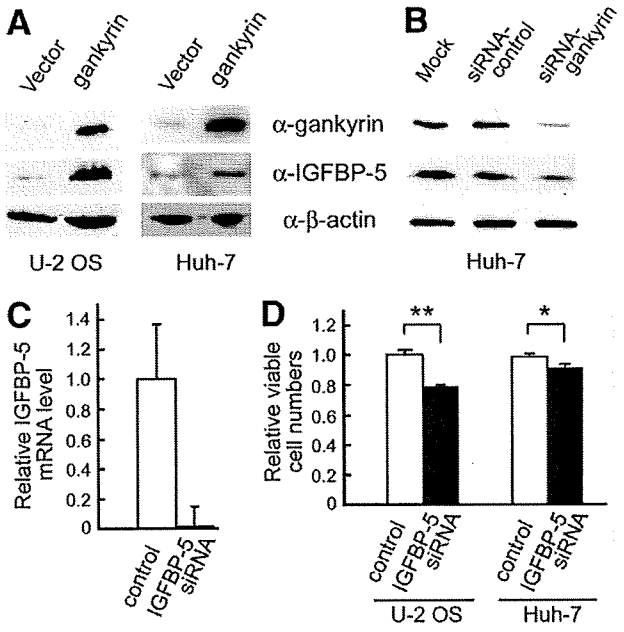

Fig. 4. Induction of IGFBP-5 by gankyrin. (A) U-2 OS cells (lanes 1 and 2) and Huh-7 cells (lanes 3 and 4) transiently transfected with plasmids expressing gankyrin or vector alone were analyzed for expression of IGFBP-5 by western blotting using the indicated antibodies. Representative results from more than 3 experiments are shown. (B) Huh-7 cells, mock transfected or transfected with siRNA for gankyrin or control RNA as indicated, were analyzed as in (A). (C) Suppression of IGFBP-5 expression by siRNA. Huh-7 cells were transfected with control RNA or IGFBP-5–specific siRNA. IGFBP-5 transcript levels were determined by real-time RT-PCR and normalized with β-actin levels. Results from 3 repeats were averaged and expressed relative to control. Error bars refer to standard deviation of the average quantitated results. (D) Effect of IGFBP-5 down-regulation on cell growth. U-2 OS and Huh-7 cells were transfected with IGFBP-5 siRNA or control RNA, and 72 hours later viable cell numbers were determined. Values are mean ± standard deviation (n = 3) and expressed relative to controls. ** and *, $P < 0.01$ and $P < 0.05$, respectively.

gankyrin (Table 3), and the levels of expression covaried both in HCCs ($\rho = 0.629$, $P < 0.001$) (Fig. 5E) and noncancerous hepatocytes ($\rho = 0.606$, $P < 0.001$) (Fig. 5F).

Expression of Gankyrin in HCC and Patient Prognosis. When we examined the relationship between gankyrin expression in HCC cells and the survival of patients after surgical resection, a significant difference was observed between the patients with gankyrin-positive HCCs and those with gankyrin-negative HCCs (Fig. 6). We found no significant difference in the survival rates between the patients whose HCCs stained positively and negatively for p53, MDM2, or IGFBP-5.

Discussion

Gankyrin is as an oncogene, mRNA of which is overexpressed in almost all human HCCs.[9,19] Although less frequent, gankyrin has been found by RNA dot blot analysis to be overexpressed in additional tumors including those of the breast, colon, rectum, stomach, small intestine, pancreas, ovary, lung, and thyroid (A. Umemura and J. Fujita, unpublished data). In the current study, we immunohistochemically examined the gankyrin protein expression in HCCs using the monoclonal anti-gankyrin antibody and found that the protein was highly expressed in the cytoplasm of 63% of HCCs. Tan et al.[20] has simi-

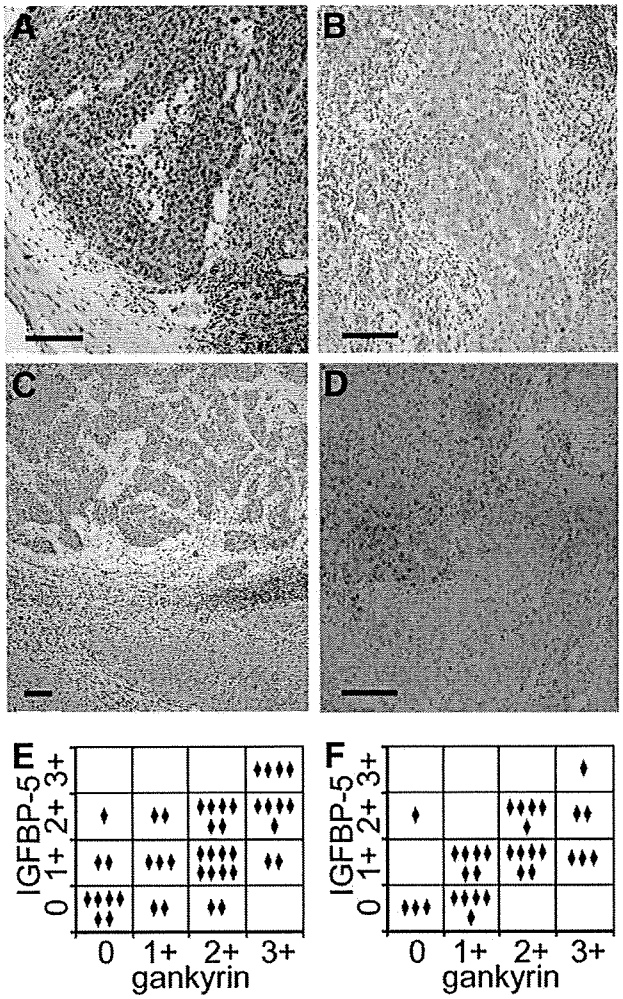

Fig. 5. Immunohistochemical detection of IGFBP-5 in hepatocellular carcinoma (HCC). HCC sections were stained with anti-IGFBP-5 antibody and counterstained with hematoxylin. Positive immunostaining appears brown. (A) Positive staining for IGFBP-5 in the cytoplasm of HCC cells, especially at the invasive boundaries. (B) Presence of IGFBP-5 in noncancerous cirrhotic hepatocytes. (C) Stronger staining for IGFBP-5 in HCC cells (upper) than the neighboring cirrhotic hepatocytes (lower). (D) Positive staining for IGFBP-5 in HCC cells (upper left), but negative in cirrhotic cells (lower right). Bar, 100 μm. (E) Correlation of expression levels of gankyrin and IGFBP-5 in HCCs. The immunostaining levels were expressed as 0 (negative), 1+ (weakly positive), 2+ (moderately positive), or 3+ (strongly positive). Each diamond represents 1 case. The Spearman's rho = 0.629, $P < 0.001$. (F) Correlation of expression levels of gankyrin and IGFBP-5 in noncancerous hepatocytes determined as in (E). The Spearman's rho = 0.606, $P < 0.001$.

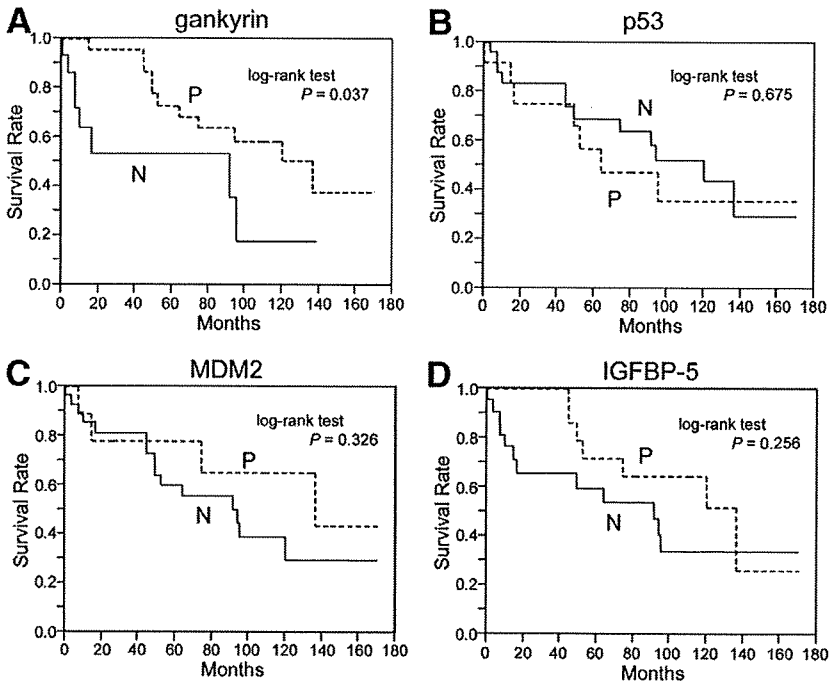

Fig. 6. Survival of patients and expression of molecular markers. The Kaplan-Meier method was used to determine the patient survival and log-rank test to compare survival between patients with HCC grouped according to (A) gankyrin positivity, (B) p53 positivity, (C) MDM2 positivity, and (D) IGFBP-5 positivity. P, positive. N, negative.

larly found overexpression of gankyrin protein in 60% of HCCs using a polyclonal antibody. The reason why the protein is not overexpressed in one-third of HCCs despite overexpression of its mRNA is unknown. The posttranscriptional, translational, and posttranslational regulations of gankyrin expression remain to be elucidated.

According to the 15th follow-up survey by the Liver Cancer Study group of Japan, the cumulative survival rates after surgical removal of HCC are 52.3% and 27.3% at 5 and 10 years, respectively, and better survival rates are associated with fewer numbers of tumors, lack of portal venous invasion, and early clinical stages.[4-6] Consistent with these observations, gankyrin positivity of HCC was associated with low TNM stage, lack of capsular invasion, portal venous invasion, and intrahepatic metastasis, and better prognosis of the patients. Patients with hyperdiploid acute lymphoblastic leukemia with more than 50 chromosomes, one of the 6 subtypes of pediatric acute lymphoblastic leukemia, have an excellent prognosis compared with other subtypes, and interestingly, overexpression of gankyrin is 1 of the diagnostic and subclassification markers for it.[21] Expression of gankyrin protein may be used as a marker for better prognosis of the patients with HCC as well.

The gankyrin oncoprotein plays a key role in regulation of cell cycle and apoptosis, at least in cultured cells, by inhibiting Rb and p53.[10] In a rodent hepatocarcinogenesis model, hypermethylation of the p16INK4A gene and p53 mutation appear at a late stage, whereas gankyrin is overexpressed from early after carcinogen treatment, preceding the loss of Rb protein and adenoma formation.[22] Clinically, p53 mutation is not so frequent in HCCs (15%-30%), especially in low-grade or low-stage HCCs.[23,24] Tan et al.[20] have immunohistochemically detected gankyrin overexpression in 82%, 63%, and 22% of Edmondson's grade I to II, III, and IV HCCs, respectively. We observed gankyrin positivity in 81% and 35% of low and high TNM stage HCCs, respectively. These results suggest that gankyrin plays an important role(s) at early stages of hepatocarcinogenesis by suppressing Rb, p53 and possibly other tumor suppressors. In advanced HCCs, by contrast, oncogenic mutations probably have accumulated in many genes including p53, and overexpression of gankyrin may not be so crucial as in early stage HCCs. This could explain the present association of gankyrin-negative HCCs with poorer prognosis and the finding that both cases of gankyrin-negative HCCs with gankyrin-positive noncancerous hepatocytes belonged to high TNM stages. This is, however, one of several possible explanations, and further work is necessary to clarify the exact reasons for the observed association.

By immunohistochemical staining, p53 has been detected in 20% to 30% of HCCs.[25, 26] Although strong immunohistochemical reactivity for p53 may not be an indicator of the presence of p53 gene mutations as initially suggested,[26] it has been associated in some studies with higher proliferative activity, lower differentiation of HCC cells, or poorer survival of patients. Endo et al.[27] immunohistochemically detected MDM2 in 28 of 107 (26%) HCCs, and the positive expression correlated with

the presence of p53 mutation and poorer prognosis, although it also correlated with smaller HCC size and the absence of vascular invasion. We immunohistochemically detected the expression of p53 and MDM2 in 30% and 23%, respectively, of HCCs, which is in accord with other studies, but no correlation was seen between expression and survival of the patients. Gankyrin accelerates degradation of Rb, p53, and MDM2 in cultured cells.[9,16] Although some correlation between expression of gankyrin and Rb has been suggested in HCC tissues,[20] we did not observe significant relationship between the gankyrin positivity and negative staining for p53 nor MDM2. The analysis of individual cells for protein expression, for example by double 2-color immunostaining, may have revealed the presence of some relationship. But most probably, our finding reflects complex interrelated mechanisms regulating the levels of these proteins and also suggests that the relevance of the effects of gankyrin on p53, MDM2, and Rb demonstrated in cultured cells to human hepatocarcinogenic process remains to be firmly established.

The 6 members of IGFBP family (IGFBP-1 through IGFBP-6) are important components of the insulin-like growth factor (IGF) axis, and regulate the activity of both IGF-I and IGF-II polypeptide growth factors.[28] IGF-I, IGF-II, and their receptors are expressed in a wide variety of cells, and the liver is the main source of circulating IGF-I. IGFBPs are also secreted by many cell types, and their expression is regulated in a cell-dependent and tissue-type–dependent manner. In the current study, we found up-regulation of IGFBP-5 mRNA and protein levels by overexpression of gankyrin in human osteosarcoma and HCC cell lines and consistently detected a significant association between the protein levels of gankyrin and IGFBP-5 in HCC specimens. In the proximal promoter region of the IGFBP-5 gene, there are several putative transcription-factor–binding sites including those for AP-2, c-Myb, C/EBP, and NF-1, and responsive elements to prostaglandin E_2, cyclic adenosine monophosphate, progesterone/retinoic acid, and Akt.[28] Whether the effect of gankyrin on IGFBP-5 expression is mediated by these factors is unknown.

The IGFBPs bind IGFs with high affinity, and they are able to enhance or inhibit the activity of IGFs in a cell-specific and tissue-type–specific manner.[28] In addition, IGFBPs have IGF-independent effects. There are several reports on the relationship between the IGF axis and HCC.[29-31] IGFBP-3 is the most abundant IGFBP present in noncancerous liver tissue and could serve as a negative regulator of cell proliferation in human HCCs.[32] Although the presence of IGFBP-5 in numerous tumors and cell lines has been demonstrated, its expression and significance in human HCC have not been documented. We found positive staining for IGFBP-5 in 42% of HCCs, and the positivity correlated with absence of portal venous invasion, low TNM stage, and small tumor size. Although not statistically significant, patients with IGFBP-5–positive HCCs tended to survive longer than those with IGFBP-5–negative HCCs. These findings are essentially similar to those observed for gankyrin. Regarding the effect of IGFBP-5 on cell proliferation, there are contradictory findings.[28] In breast cancer cells, many studies have reported inhibition of growth, but there are some indicating a stimulatory effect.[33] IGFBP-5 is up-regulated in involuting prostate but is also implicated in growth stimulation of prostate tumor cells.[34] We found that down-regulation of IGFBP-5 suppresses growth of Huh-7 HCC cells. Thus, these findings are consistent with a notion that high expression of IGFBP-5 and gankyrin play oncogenic roles in HCCs of early clinical stages. Clarification of the exact roles played by them will shed more light on the molecular mechanisms of human hepatocarcinogenesis and lead to development of new therapeutic and preventive strategies.

Acknowledgment: We thank Dr. R. John Mayer for helpful suggestions.

References

1. Parkin DM, Bray F, Ferlay J, Pisani P. Global cancer statistics, 2002. CA Cancer J Clin 2005;55:74-108.
2. Thomas MB, Zhu AX. Hepatocellular carcinoma: the need for progress. J Clin Oncol 2005;23:2892-2899.
3. Treiber G, Wex T, Rocken C, Fostitsch P, Malfertheiner P. Impact of biomarkers on disease survival and progression in patients treated with octreotide for advanced hepatocellular carcinoma. J Cancer Res Clin Oncol 2006;132:699-708.
4. Shimada K, Sano T, Sakamoto Y, Kosuge T. A long-term follow-up and management study of hepatocellular carcinoma patients surviving for 10 years or longer after curative hepatectomy. Cancer 2005;104:1939-1947.
5. Poon RT, Fan ST, Ng IO, Lo CM, Liu CL, Wong J. Different risk factors and prognosis for early and late intrahepatic recurrence after resection of hepatocellular carcinoma. Cancer 2000;89:500-507.
6. Kiyosawa K, Umemura T, Ichijo T, Matsumoto A, Yoshizawa K, Gad A, et al. Hepatocellular carcinoma: recent trends in Japan. Gastroenterology 2004;127(5 Suppl 1):S17-S26.
7. Higashitsuji H, Higashitsuji H, Nagao T, Nonoguchi K, Fujii S, Itoh K, et al. A novel protein overexpressed in hepatoma accelerates export of NF-kappa B from the nucleus and inhibits p53-dependent apoptosis. Cancer Cell 2002;2:335-346.
8. Gotoh K, Nonoguchi K, Higashitsuji H, Kaneko Y, Sakurai T, Sumitomo Y, et al. Apg-2 has a chaperone-like activity similar to Hsp110 and is overexpressed in hepatocellular carcinomas. FEBS Lett 2004;560:19-24.
9. Higashitsuji H, Itoh K, Nagao T, Dawson S, Nonoguchi K, Kido T, et al. Reduced stability of retinoblastoma protein by gankyrin, an oncogenic ankyrin-repeat protein overexpressed in hepatomas. Nat Med 2000;6:96-99.
10. Higashitsuji H, Liu Y, Mayer RJ, Fujita J. The oncoprotein gankyrin negatively regulates both p53 and RB by enhancing proteasomal degradation. Cell Cycle 2005;4:1335-1337.
11. Hori T, Kato S, Saeki M, DeMartino GN, Slaughter CA, Takeuchi J, et al. cDNA cloning and functional analysis of p28 (Nas6p) and p40.5 (Nas7p),

two novel regulatory subunits of the 26S proteasome. Gene 1998;216:113-122.
12. Dawson S, Apcher S, Mee M, Higashitsuji H, Baker R, Uhle S, et al. Gankyrin is an ankyrin-repeat oncoprotein that interacts with CDK4 kinase and the S6 ATPase of the 26 S proteasome. J Biol Chem 2002;277: 10893-10902.
13. Li J, Tsai MD. Novel insights into the INK4-CDK4/6-Rb pathway: counter action of gankyrin against INK4 proteins regulates the CDK4-mediated phosphorylation of Rb. Biochemistry 2002;41:3977-3983.
14. Shan YF, Zhou WP, Fu XY, Yan HX, Yang W, Liu SQ, et al. The role of p28GANK in rat oval cells activation and proliferation. Liver Int 2006;26: 240-247.
15. Iwai A, Marusawa H, Kiuchi T, Higashitsuji H, Tanaka K, Fujita J, et al. Role of a novel oncogenic protein, gankyrin, in hepatocyte proliferation. J Gastroenterol 2003;38:751-758.
16. Higashitsuji H, Higashitsuji H, Itoh K, Sakurai T, Nagao T, Sumitomo Y, et al. The oncoprotein gankyrin binds to MDM2/HDM2, enhancing ubiquitylation and degradation of p53. Cancer Cell 2005;8:75-87.
17. Ueno S, Tanabe G, Nuruki K, Hamanoue M, Komorizono Y, Oketani M, et al. Prognostic performance of the new classification of primary liver cancer of Japan (4th edition) for patients with hepatocellular carcinoma: a validation analysis. Hepatol Res 2002;24:395-403.
18. Desmet VJ. Histological classification of chronic hepatitis. Acta Gastroenterol Belg 1997;60:259-267.
19. Fu XY, Wang HY, Tan L, Liu SQ, Cao HF, Wu MC. Overexpression of p28/gankyrin in human hepatocellular carcinoma and its clinical significance. World J Gastroenterol 2002;8:638-643.
20. Tan L, Fu XY, Liu SQ, Li HH, Hong Y, Wu MC, et al. Expression of p28GANK and its correlation with RB in human hepatocellular carcinoma. Liver Int 2005;25:667-676.
21. Yeoh EJ, Ross ME, Shurtleff SA, Williams WK, Patel D, Mahfouz R, et al. Classification, subtype discovery, and prediction of outcome in pediatric acute lymphoblastic leukemia by gene expression profiling. Cancer Cell 2002;1:133-143.
22. Park TJ, Kim HS, Byun KH, Jang JJ, Lee YS, Lim IK. Sequential changes in hepatocarcinogenesis induced by diethylnitrosamine plus thioacetamide in Fischer 344 rats: induction of gankyrin expression in liver fibrosis, pRB degradation in cirrhosis, and methylation of p16(INK4A) exon 1 in hepatocellular carcinoma. Mol Carcinog 2001;30:138-150.
23. Tanaka S, Toh Y, Adachi E, Matsumata T, Mori R, Sugimachi K. Tumor progression in hepatocellular carcinoma may be mediated by p53 mutation. Cancer Res 1993;53:2884-2887.
24. Hayashi H, Sugio K, Matsumata T, Adachi E, Takenaka K, Sugimachi K. The clinical significance of p53 gene mutation in hepatocellular carcinomas from Japan. HEPATOLOGY 1995;22:1702-1707.
25. Nagao T, Kondo F, Sato T, Nagato Y, Kondo Y. Immunohistochemical detection of aberrant p53 expression in hepatocellular carcinoma: correlation with cell proliferative activity indices, including mitotic index and MIB-1 immunostaining. Hum Pathol 1995;26:326-333.
26. Anzola M, Saiz A, Cuevas N, Lopez-Martinez M, Martinez de Pancorbo MA, Burgos JJ, et al. High levels of p53 protein expression do not correlate with p53 mutations in hepatocellular carcinoma. J Viral Hepat 2004;11: 502-510.
27. Endo K, Ueda T, Ohta T, Terada T. Protein expression of MDM2 and its clinicopathological relationships in human hepatocellular carcinoma. Liver 2000;20:209-215.
28. Beattie J, Allan GJ, Lochrie JD, Flint DJ. Insulin-like growth factor-binding protein-5 (IGFBP-5): a critical member of the IGF axis. Biochem J 2006;395:1-19.
29. Gong Y, Cui L, Minuk GY. The expression of insulin-like growth factor binding proteins in human hepatocellular carcinoma. Mol Cell Biochem 2000;207:101-104.
30. Scharf JG, Dombrowski F, Ramadori G. The IGF axis and hepatocarcinogenesis. Mol Pathol 2001;54:138-144.
31. Breuhahn K, Longerich T, Schirmacher P. Dysregulation of growth factor signaling in human hepatocellular carcinoma. Oncogene 2006;25:3787-3800.
32. Huynh H, Chow PK, Ooi LL, Soo KC. A possible role for insulin-like growth factor-binding protein-3 autocrine/paracrine loops in controlling hepatocellular carcinoma cell proliferation. Cell Growth Differ 2002;13: 115-122.
33. McCaig C, Perks CM, Holly JM. Intrinsic actions of IGFBP-3 and IGFBP-5 on Hs578T breast cancer epithelial cells: inhibition or accentuation of attachment and survival is dependent upon the presence of fibronectin. J Cell Sci 2002;115:4293-4303.
34. Miyake H, Pollak M, Gleave ME. Castration-induced up-regulation of insulin-like growth factor binding protein-5 potentiates insulin-like growth factor-I activity and accelerates progression to androgen independence in prostate cancer models. Cancer Res 2000;60:3058-3064.

Int. J. Cancer: **122,** 2148–2153 (2008)

Synergistic antitumor activity of the novel SN-38-incorporating polymeric micelles, NK012, combined with 5-fluorouracil in a mouse model of colorectal cancer, as compared with that of irinotecan plus 5-fluorouracil

Takako Eguchi Nakajima[1,2], Masahiro Yasunaga[2], Yasuhiko Kano[3], Fumiaki Koizumi[4], Ken Kato[1], Tetsuya Hamaguchi[1], Yasuhide Yamada[1], Kuniaki Shirao[1], Yasuhiro Shimada[1] and Yasuhiro Matsumura[2]*

[1]*Gastrointestinal Oncology Division, National Cancer Center Hospital, Tokyo, Japan*
[2]*Investigative Treatment Division, Research Center for Innovative Oncology, National Cancer Center Hospital East, Kashiwa, Chiba, Japan*
[3]*Hematology Oncology, Tochigi Cancer Center, Tochigi, Japan*
[4]*Shien Lab Medical Oncology Division, National Cancer Center Hospital, Tokyo, Japan*

The authors reported in a previous study that NK012, a 7-ethyl-10-hydroxy-camptothecin (SN-38)-releasing nano-system, exhibited high antitumor activity against human colorectal cancer xenografts. This study was conducted to investigate the advantages of NK012 over irinotecan hydrochloride (CPT-11) administered in combination with 5-fluorouracil (5FU). The cytotoxic effects of NK012 or SN-38 (an active metabolite of CPT-11) administered in combination with 5FU was evaluated *in vitro* in the human colorectal cancer cell line HT-29 by the combination index method. The effects of the same drug combinations was also evaluated *in vivo* using mice bearing HT-29 and HCT-116 cells. All the drugs were administered i.v. 3 times a week; NK012 (10 mg/kg) or CPT11 (50 mg/kg) was given 24 hr before 5FU (50 mg/kg). Cell cycle analysis in the HT-29 tumors administered NK012 or CPT-11 *in vivo* was performed by flow cytometry. NK012 exerted more synergistic activity with 5FU compared to SN-38. The therapeutic effect of NK012/5FU was significantly superior to that of CPT-11/5FU against HT-29 tumors ($p = 0.0004$), whereas no significant difference in the antitumor effect against HCT-116 tumors was observed between the 2-drug combinations ($p = 0.2230$). Cell-cycle analysis showed that both NK012 and CPT-11 tend to cause accumulation of cells in the S phase, although this effect was more pronounced and maintained for a more prolonged period with NK012 than with CPT-11. Optimal therapeutic synergy was observed between NK012 and 5FU, therefore, this regimen is considered to hold promise of clinical benefit, especially for patients with colorectal cancer.

Key words: NK012; SN-38; 5-fluorouracil; drug delivery system; colorectal cancer

The 5-year survival rates of colorectal cancer (CRC) have improved remarkably over the last 10 years, accounted for in large part by the extensively investigated agents after 5-fluorouracil (5FU). Irinoetcan hydrochloride (CPT-11), a water-soluble, semi-synthetic derivative of camptothecin, is one such agent that has been shown to be highly effective, and currently represents a key-drug in first- and second-line treatment regimens for CRC. CPT-11 monotherapy, however, has not been shown to yield superior efficacy, including in terms of the median survival time, to bolus 5FU/leucovorin (LV) alone.[1] In 2 Phase III trials, the addition of CPT-11 to bolus or infusional 5FU/LV regimens clearly yielded greater efficacy than administration of 5FU/LV alone, with a doubling of the tumor response rate and prolongation of the median survival time by 2–3 months.[1,2]

CPT-11 is converted to 7-ethyl-10-hydroxy-camptothecin (SN-38), a biologically active and water-insoluble metabolite of CPT-11, by carboxylesterases in the liver and the tumor. SN-38 has been demonstrated to exhibit up to a 1,000-fold more potent cytotoxic activity than CPT-11 against various cancer cells *in vitro*.[3] The metabolic conversion rate is, however, very low, with only <10% of the original volume of CPT-11 being metabolized to SN-38[4,5]; conversion of CPT-11 to SN-38 also depends on genetic interindividual variability of the activity of carboxylesterases.[6] Direct use of SN-38 itself for clinical cancer treatment must be shown to be identical in terms of both efficacy and toxicity.

Some drugs incorporated in drug delivery systems (DDS), such as Abraxane and Doxil, are already in clinical use.[7,8] The clinical benefits of DDS are based on their EPR effect.[9] The EPR effect is based on the pathophysiological characteristics of solid tumor tissues: hypervascularity, incomplete vascular architecture, secretion of vascular permeability factors stimulating extravasation within cancer tissue, and absence of effective lymphatic drainage from the tumors that impedes the efficient clearance of macromolecules accumulated in solid tumor tissues. Several types of DDS can be used for incorporation of a drug. A liposome-based formulation of SN-38 (LE-SN38) has been developed, and a clinical trial to assess its efficacy is now under way.[10,11]

Recently, we demonstrated that NK012, novel SN-38-incorporating polymeric micelles, exerted superior antitumor activity and less toxicity than CPT-11.[12] NK012 is characterized by a smaller size of the particles than LE-SN38; the mean particle diameter of NK012 is 20 nm. NK012 can release SN-38 under neutral conditions even in the absence of a hydrolytic enzyme, because the bond between SN-38 and the block copolymer is a phenol ester bond, which is stable under acidic conditions and labile under mild alkaline conditions. The release rate of SN-38 from NK012 under physiological conditions is quite high; more than 70% of SN-38 is released within 48 hr. We speculated that the use of NK012, in place of CPT-11, in combination with 5FU may yield superior results in the treatment of CRC. In the present study, we evaluated the antitumor activity of NK012 administered in combination with 5FU as compared to that of CPT-11 administered in combination with 5FU against CRC in an experimental model.

Material and methods

Cells and animals

The human colorectal cancer cell lines used, namely, HT-29 and HCT-116, were purchased from the American Type Culture Collection (Rockville, MD). The HT-29 cells and HCT-116 cells were maintained in RPMI 1640 supplemented with 10% fetal bovine serum (Cell Culture Technologies, Gaggenau-Hoerden, Germany), penicillin, streptomycin, and amphotericin B (100 units/mL, 100 μg/mL, and 25 μg/mL, respectively; Sigma, St. Louis, MO) in a humidified atmosphere containing 5% CO_2 at 37°C.

BALB/c *nu/nu* mice were purchased from SLC Japan (Shizuoka, Japan). Six-week-old mice were subcutaneously (s.c.)

***Correspondence to:** Investigative Treatment Division, Research Center for Innovative Oncology, National Cancer Center Hospital East, 6-5-1 Kashiwanoha, Kashiwa, Chiba 277-8577, Japan. Fax: +81-4-7134-6866. E-mail: yhmatsum@east.ncc.go.jp
Received 2 September 2007; Accepted after revision 20 November 2007
DOI 10.1002/ijc.23381
Published online 14 January 2008 in Wiley InterScience (www.interscience.wiley.com).

inoculated with 1×10^6 cells of HT-29 or HCT-116 cell line in the flank region. The length (*a*) and width (*b*) of the tumor masses were measured twice a week, and the tumor volume (TV) was calculated as follows: $TV = (a \times b^2)/2$. All animal procedures were performed in compliance with the Guidelines for the Care and Use of Experimental Animals established by the Committee for Animal Experimentation of the National Cancer Center; these guidelines meet the ethical standards required by law and also comply with the guidelines for the use of experimental animals in Japan.

Drugs

The SN-38-incorporating polymeric micelles, NK012, and SN-38 were prepared by Nippon Kayaku (Tokyo, Japan).[12] CPT-11 was purchased from Yakult Honsha (Tokyo, Japan). 5FU was purchased from Kyowa Hakko (Tokyo, Japan).

Cell growth inhibition assay

HT-29 cells were seeded in 96-well plates at a density of 2,000 cells/well in a final volume of 90 μL. Twenty-four hours after seeding, a graded concentration of NK012 or SN-38 was added concurrently with 5FU to the culture medium of the HT-29 cells in a final volume of 100 μL for drug interaction studies. The culture was maintained in the CO_2 incubator for an additional 72 hr. Then, cell growth inhibition was measured by the tetrazolium salt-based proliferation assay (WST assay; Wako Chemicals, Osaka, Japan). WST-1 labeling solution (10 μL) was added to each well and the plates were incubated at 37°C for 3 hr. The absorbance of the formazan product formed was detected at 450 nm in a 96-well spectrophotometric plate reader. Cell viability was measured and compared to that of the control cells. Each experiment was carried out in triplicate and was repeated at least 3 times. Data were averaged and normalized against the nontreated controls to generate dose-response curves.

Drug interaction analysis

The nature of interaction between NK012 or SN-38 and 5FU against HT-29 cells was evaluated by median-effect plot analyses and the combination index (CI) method of Chou and Talalay.[13] Data analysis was performed using the Calcusyn software (Biosoft, NY, USA). NK012 or SN-38 was combined with 5FU at a fixed ratio that spanned the individual IC_{50} values of each drug. The IC_{50} values were determined on the basis of the dose-response curves using the WST assay. For any given drug combination, the CI is known to represent the degree of synergy, additivity or antagonism. It is expressed in terms of fraction-affected (*Fa*) values, which represents the percentage of cells killed or inhibited by the drug. Isobologram equations and *Fa*/CI plots were constructed by computer analysis of the data generated from the median effect analysis. Each experiment was performed in triplicate with 6 gradations and was repeated at least 3 times. The resultant dose-response curves were averaged, to create a single composite dose-response curve for each combination.

In vivo analysis of the effects of NK012 combined with 5FU as compared to those of CPT-11 combined with 5FU

When the mean tumor volumes reached ~93 mm^3, the mice were randomly divided into test groups consisting of 5 mice per group (Day 0). The drugs were administered i.v. *via* the tail vein of the mice. In the groups administered NK012 or 5FU as single agents, the drug was administered on Days 0, 7 and 14. In the combined treatment groups, NK012 or CPT-11 was administered 24 hr before 5FU on Days 0, 7 and 14, according to the previously reported combination schedule for CPT-11 and 5FU.[14] Complete response (CR) was defined as tumor not detectable by palpation at 90 days after the start of treatment, at which time-point the mice were sacrificed. Tumor volume and body weight were measured twice a week. As a general rule, animals in which the tumor volume exceeded 2,000 mm^3 were also sacrificed.

Experiment 1. Evaluation of the effects of NK012 combined with 5FU and determination of the maximum tolerated dose (MTD) of NK012/5FU. By comparing the data between NK012 administered as a single agent and NK012/5FU, we evaluated the effects of the combined regimen against the s.c HT-29 tumors. A preliminary experiment showed that combined administration of NK012 15 mg/kg + 5FU 50 mg/kg every 6 days caused drug-related lethality (data not shown). To determine the MTD, therefore, we set the dosing schedule of the combined regimen at 5 or 10 mg/kg of NK012 + 50 mg/kg of 5FU three times a week.

Experiment 2. Comparison of the antitumor effect of NK012/5FU and CPT-11/5FU. Based on a comparison of the data between NK012/5FU and CPT-11/5FU against the s.c. HT-29 and HCT-116 tumors, we investigated the feasibility of the clinical application of NK012/5FU for the treatment of CRC. CPT-11/5FU was administered three times a week at the respective MTDs of the 2 drugs as previously reported, that is, CPT11 at 50 mg/kg and 5FU at 50 mg/kg, respectively.[14] NK012/5FU was administered once three times a week at the respective MTDs of the 2 drugs determined from Experiment 1.

Cell cycle analysis

Samples from the HT-29 tumors that had grown to 80–100 mm^3 were removed from the mice at 6, 24, 48, 72 and 96 hr after the administration of NK012 alone at 10 mg/kg or CPT-11 alone at 50 mg/kg. The samples were excised, minced in PBS and fixed in 70% ethanol at −20°C for 48 hr. They were then digested with 0.04% pepsin (Sigma chemical Co., St Lous, MO) in 0.1 N HCL for 60 min at 37°C in a shaking bath to prepare single-nuclei suspensions. The nuclei were then centrifuged, washed twice with PBS and stained with 40 μg/mL of propidium iodide (Molecular Probes, OR) in the presence of 100 μg/mL RNase in 1 mL PBS for 30 min at 37°C. The stained nuclei were analyzed with B-D FACSCalibur (BD Biosciences, San Jose, CA), and the cell cycle distribution was analyzed using the Modfit program (Verity Software House Topsham, ME).

Statistical analyses

Data were expressed as mean ± SD. Data were analysed with Student's *t* test when the groups showed equal variances (*F* test), or Welch's test when they showed unequal variances (*F* test). $p < 0.05$ was regarded as statistically significant. All statistical tests were 2-sided.

Results

Antiproliferative effects of NK012 or SN-38 administered in combination with 5FU

Figure 1*a* shows the dose-response curves for NK012 alone, 5FU alone and a combination of the two. The IC_{50} levels of NK012 and 5FU against the HT-29 cells were 39 nM and 1 μM, respectively, and the IC_{50} level of SN-38 was 14 nM (data not shown). Based on these data, the molar ratio of NK012 or SN-38:5FU of 1:1,000 was used for the drug combination studies.

Figures 1*b* and 1*c* show the median-effect and the combination index plots. Combination indices (CIs) of <1.0 are indicative of synergistic interactions between 2 agents; additive interactions are indicated by CIs of 1.0, and antagonism by CIs of >1.0. Figure 1*c* shows the combination index for NK012 and 5FU, when 2 drugs are supposed to be mutually exclusive. Marked synergism was observed between Fa 0.2 and 0.6. Theoretically, the CI method is the most reliable around an Fa of 0.5, suggesting synergistic effects of the combination of NK012 and 5FU. This synergistic effect was more evident than that of SN-38/5FU (Fig. 1*d*).

In vivo *effect of combined NK012 and 5FU*

Experiment 1. Dose optimization and effect of combined NK012 and 5FU against HT-29 tumors. Comparison of the relative tumor volumes on Day 40 revealed significant differences between

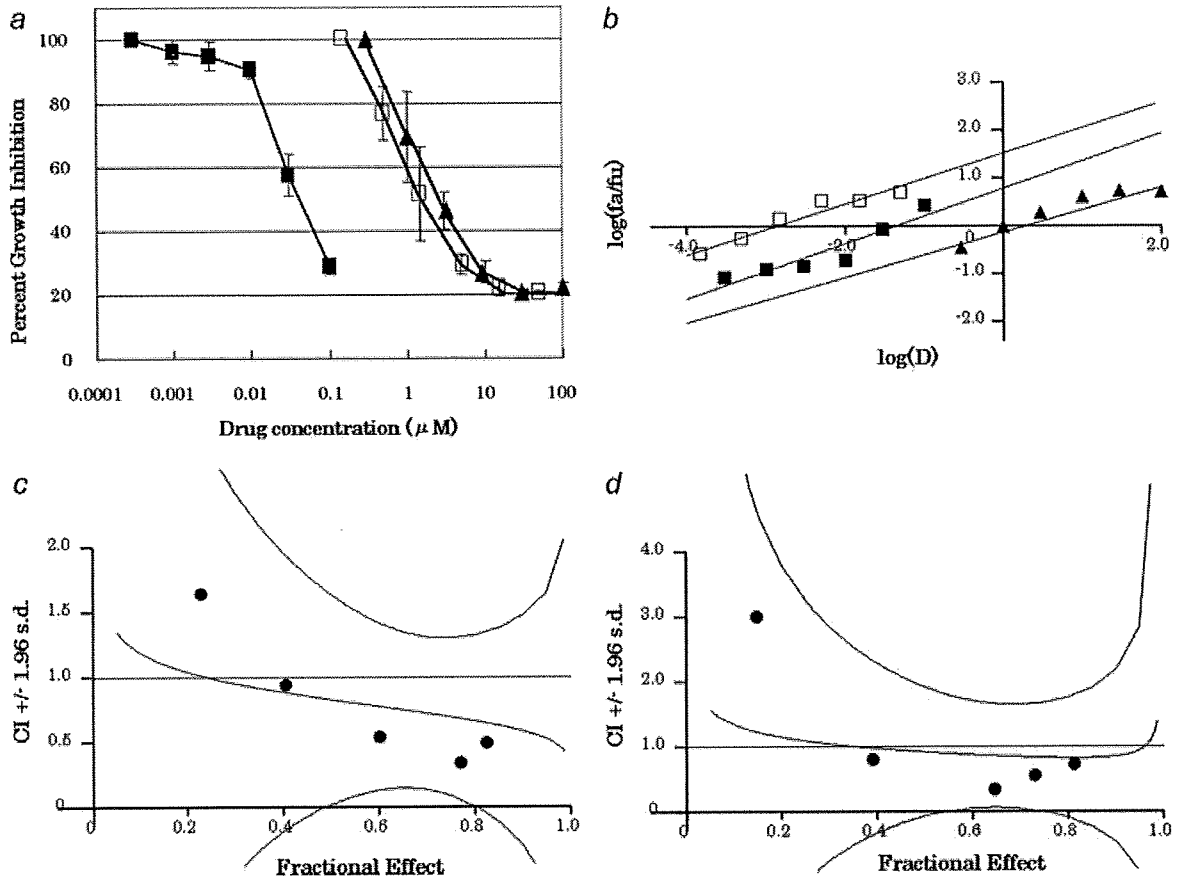

FIGURE 1 – Interaction of NK012 and 5FU *in vitro*. (*a*) Dose-response curves for NK012 alone (■), 5FU alone (▲) and their combination (□) against HT-29 cells. HT-29 cells were seeded at 2,000 cells/well. Twenty-four hours after seeding, a graded concentration of NK012 or 5FU was added to the culture medium of the HT-29 cells. Cell growth inhibition was measured by WST assay after 72 hr of treatment. Cell viability was measured and compared with that of the control cells. Each experiment was carried out independently and repeated at least 3 times. Points, mean of tripricates; bars, SD. (*b*) Median effect plot for the interaction of NK012 and 5FU. (*c*, *d*) Combination index for the interaction as a function of the level of effect (fraction effect = 0.5 is the IC_{50}). The straight line across the CI value of 1.0 indicates additive effect and CIs above and below indicate antagonism and synergism, respectively. The molar ratio of NK012/5FU (*c*) or SN-38/5FU (*d*) at 1:1,000 was tested by CI analysis. Black circles represent the CIs of the actual data points, solid lines represent the computer-derived CIs at effect levels ranging from 10 to 100% inhibition of cell growth, and the dotted lines represent the 95% confidence intervals.

those in the mice administered NK012 alone and those administered NK012/5FU at 5 mg/kg of NK012 ($p = 0.018$) (Fig. 2*a*). Although there was no statistically significant difference in the relative tumor volume measured on Day 54 between the mice administered NK012 alone and NK012/5FU at 10 mg/kg of NK012 ($p = 0.3050$), a trend of superior antitumor effect was demonstrated in the group treated with NK012/5FU at 10 mg/kg of NK012 (Fig. 2*a*). The CR rates were 20, 40 and 60% for 5 mg/kg NK012 + 50 mg/kg 5FU, 10 mg/kg NK012 alone and 10 mg/kg NK012 + 50 mg/kg 5FU, respectively. The schedule of 10 mg/kg NK012 + 50 mg/kg 5FU resulted in no remarkable toxicity in terms of body weight changes, and these doses were determined as representing the MTDs (Fig. 2*b*).

Experiment 2. Comparison of the antitumor effect of combined NK012/5FU and CPT-11/5FU against HT-29 and HCT-116 tumors. The therapeutic effect of NK012/5FU on Day 60 was significantly superior to that of CPT-11/5FU against the HT-29 tumors ($p = 0.0004$) (Fig. 3*a*). A more potent antitumor effect, namely, a 100% CR rate, was obtained in the NK012/5FU group as compared to the 0% CR rate in the CPT-11/5FU group. Although no statistically significant difference in the relative tumor volume on Day 61 was demonstrated between the NK012/5FU and CPT-11/5FU in the case of the HCT-116 tumors ($p = 0.2230$), a trend of superior antitumor effect against these tumors was observed in the NK012/5FU treatment group (Fig. 3*b*). The CR rates for the case of the HCT-116 tumors were 0% in both NK012/5FU and CPT-11/5FU groups.

Specificity of cell cycle perturbation

We studied the differences in the effects between NK012 10 mg/kg and CPT-11 50 mg/kg on the cell cycle (Fig. 4*a*). The data indicated that both NK012 and CPT-11 tended to cause accumulation of cells in the S phase, although the effect of NK012 was stronger and maintained for a more prolonged period than that of CPT-11; the maximal percentage of S-phase cells in the total cell population in the tumors was 34% at 24 hr after the administration of CPT-11, whereas it was 39% at 48 hr after the administration of NK012 (Figs. 4*b*, and 4*c*).

Discussion

Our primary endpoint was to clarify the advantages of NK012 over CPT-11 administered in combination with 5FU. We demonstrated that combined NK012 and 5FU chemotherapy exerts more

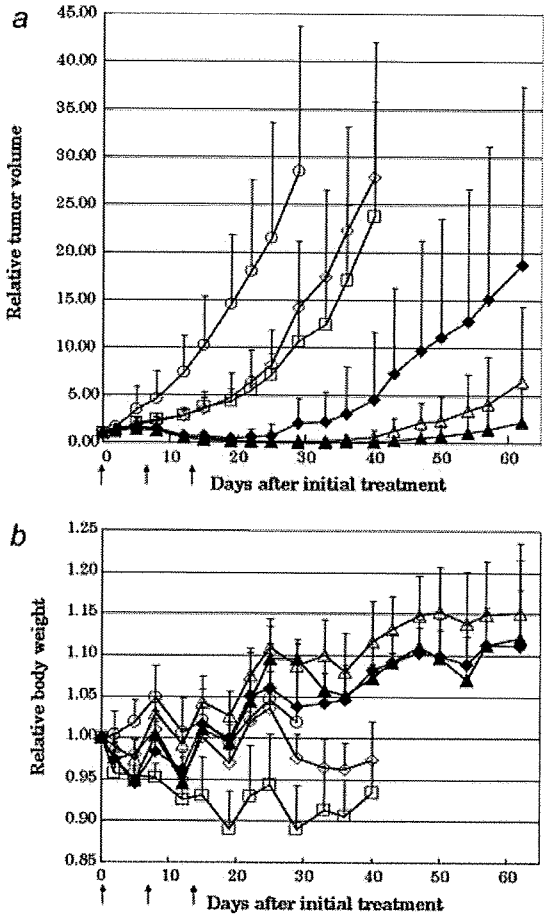

FIGURE 2 – Effect of NK012 alone or NK012 in combination with 5FU against HT-29 tumor-bearing mice. Points, mean; bars, SD. (*a*) Antitumor effect of each regimen on Days 0, 7 and 14. (○) control, (□) 5FU 50 mg/kg alone, (◇) NK012 5 mg/kg alone, (◆) NK012 5 mg/kg 24 hr before 5FU 50 mg/kg, (△) NK012 10 mg/kg alone, (▲) NK012 10 mg/kg 24 hr before 5FU 50 mg/kg. (*b*) Changes in the relative body weight. Data were derived from the same mice as those used in the present study.

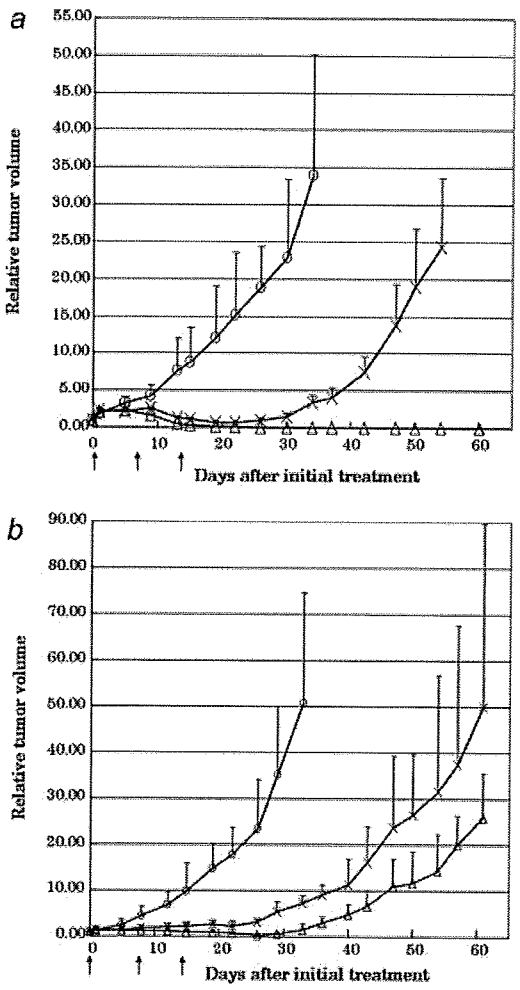

FIGURE 3 – Effect of NK012/5FU as compared with that of CPT11/5FU against HT-29 (*a*) or HCT-116 (*b*) tumor-bearing mice. Antitumor effect of each schedule on Days 0, 7 and 14. (○) control, (×) CPT-11 50 mg/kg 24 hr before 5FU 50 mg/kg, (△) NK012 10 mg/kg 24 hr before 5FU 50 mg/kg. Points, mean; bars, SD.

synergistic activity *in vitro* and significantly greater antitumor activity against human CRC xenografts as compared to CPT-11/5FU. The combination of NK012 and 5FU is considered to hold promise of clinical benefit for patients with CRC.

CPT-11, a topoisomerase-I inhibitor, and 5FU, a thymidilate synthase inhibitor, have been demonstrated to be effective agents for the treatment of CRC. A combination of these 2 drugs has also been demonstrated to be clearly more effective than either CPT-11 or 5FU/LV administered alone *in vivo* and in clinical settings.[1,2,14] Administration of 5FU by infusion with CPT-11 was shown to be associated with reduced toxicity and an apparent improvement in survival as compared to that of administration of the drug by bolus injection with CPT-11.[1,2] This synergistic enhancement may result from the mechanism of action of the 2 drugs; CPT-11 has been reported to cause accumulation of cells in the S phase, and 5FU infusion is known to cause DNA damage specifically in cells of the S phase.[14] On the basis of this background, our results suggesting the more pronounced and more prolonged accumulation of the tumor cells in the S phase caused by NK012 as compared with that by CPT-11 may explain the more effective synergy of the former administered with 5FU infusion. This may be attributable to accumulation of NK012 due to the enhanced permeability and retention (EPR) effect.[9] It is also speculated that NK012 allows sustained release of free SN-38, which may move more freely in the tumor interstitium.[15] Otherwise NK012 itself could internalize into cells to localize in several cytoplasmic organelles as reported by Savic *et al.*[16] These characteristics of NK012 may be responsible for its more potent antitumor activity observed in this study, because CPT-11 has been reported to show time-dependent growth-inhibitory activity against the tumor cells.[17]

The major dose-limiting toxicities of CPT-11 are diarrhea and neutropenia. SN-38, the active metabolite of CPT-11, may cause CPT-11-related diarrhea as a result of mitotic -inhibitory activity.[18] Because it undergoes significant biliary excretion, SN-38 may have a potentially long residence time in the gastrointestinal tract that may be associated with prolonged diarrhea.[19,20] In our previous report, we evaluated the tissue distribution of SN-38 after administration of an equimolar amount of NK012 (20 mg/kg) and CPT-11 (30 mg/kg), and found no difference in the level of SN-38 accumulation in the small intestine.[12] A significant antitumor effect of NK012 with a lower incidence of diarrhea was also dem-

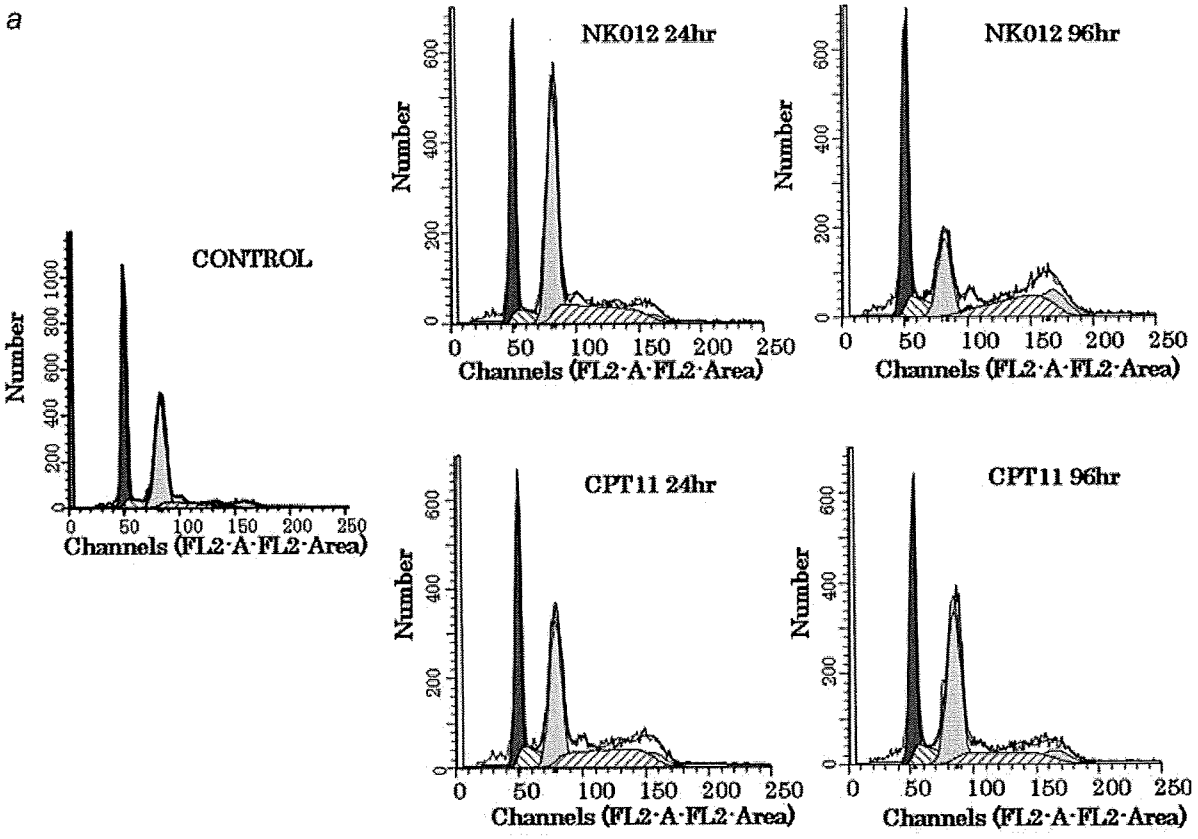

FIGURE 4 – Cell cycle analysis of HT-29 tumor cells collected 24, 48, 72 and 96 hr after administration of NK012 at 10 mg/kg alone or CPT-11 at 50 mg/kg alone using the Modfit program (Verity Software House Topsham, ME). (*a*) Cell cycle analysis of HT-29 tumor cells 24 and 96 hr after administration of NK012 at 10 mg/kg or CPT-11 at 50 mg/kg, respectively. (*b*) Cell cycle distribution of tumor cells 0, 24, 48, 72 and 96 hr after treatment with NK012 at 10 mg/kg. (*c*) Cell cycle distribution of tumor cells 0, 24, 48, 72 and 96 hr after treatment with CPT-11 at 50 mg/kg.

onstrated as compared to that observed with CPT-11 in a rat mammary tumor model.[21] Combined administration of CPT-11 with 5FU/LV infusion appears to be associated with acceptable toxicity in patients with CRC. In addition, no significant difference in the frequency of Grade 3/4 diarrhea was noted between patients treated with FOLFIRI (CPT-11 regimen with bolus and infusional 5FU/LV) and those treated with FOLFOX6 (oxaliplatin regimen with bolus and infusional 5FU/LV).[22,23] Our *in vivo* data actually revealed no severe body weight loss in the NK012/5FU group. Consequently, we expect that the NK012/5FU regimen, especially

with infusional 5FU, may be an attractive arm for a Phase III trial in CRC, with CPT-11/5FU as the control arm. We have already initiated a Phase I trial of NK012 in patients with advanced solid tumors based on the data suggesting higher efficacy and lower toxicity of this preparation than CPT-11 *in vivo*.[12]

In conclusion, we demonstrated that combined NK012 and 5FU chemotherapy exerts significantly greater antitumor activity against human CRC xenografts as compared to CPT-11/5FU, indicating the necessity of clinical evaluation of this combined regimen.

References

1. Saltz LB, Douillard JY, Pirotta N, Alakl M, Gruia G, Awad L, Elfring GL, Locker PK, Miller LL. Irinotecan plus fluorouracil/leucovorin for metastatic colorectal cancer: a new survival standard. Oncologist 2001;6:81–91.
2. Douillard JY, Cunningham D, Roth AD, Navarro M, James RD, Karasek P, Jandik P, Iveson T, Carmichael J, Alakl M, Gruia G, Awad L, et al. Irinotecan combined with fluorouracil compared with fluorouracil alone as first-line treatment for metastatic colorectal cancer: a multicentre randomised trial. Lancet 2000;355:1041–7.
3. Takimoto CH, Arbuck SG. Topoisomerase I targeting agents: the camptothecins. In: Chabner BA, Lango DL, eds. Cancer chemotherapy and biotherapy: principal and practice, 3rd ed. Philadelphia, PA: Lippincott Williams and Wilkins, 2001. 579–646.
4. Slatter JG, Schaaf LJ, Sams JP, Feenstra KL, Johnson MG, Bombardt PA, Cathcart KS, Verburg MT, Pearson LK, Compton LD, Miller LL, Baker DS, et al. Pharmacokinetics, metabolism, and excretion of irinotecan (CPT-11) following I.V. infusion of [(14)C]CPT-11 in cancer patients. Drug Metab Dispos 2000;28:423–33.
5. Rothenberg ML, Kuhn JG, Burris HA, III, Nelson J, Eckardt JR, Tristan-Morales M, Hilsenbeck SG, Weiss GR, Smith LS, Rodriguez GI, Rock MK, Von Hoff DD. Phase I and pharmacokinetic trial of weekly CPT-11. J Clin Oncol 1993;11:2194–204.
6. Guichard S, Terret C, Hennebelle I, Lochon I, Chevreau P, Fretigny E, Selves J, Chatelut E, Bugat R, Canal P. CPT-11 converting carboxylesterase and topoisomerase activities in tumour and normal colon and liver tissues. Br J Cancer 1999;80:364–70.
7. Gradishar WJ, Tjulandin S, Davidson N, Shaw H, Desai N, Bhar P, Hawkins M, O'Shaughnessy J. Phase III trial of nanoparticle albumin-bound paclitaxel compared with polyethylated castor oil-based paclitaxel in women with breast cancer. J Clin Oncol 2005;23:7794–803.
8. Muggia FM. Liposomal encapsulated anthracyclines: new therapeutic horizons. Curr Oncol Rep 2001;3:156–62.
9. Matsumura Y, Maeda H. A new concept for macromolecular therapeutics in cancer chemotherapy: mechanism of tumoritropic accumulation of proteins and the antitumor agent smancs. Cancer Res 1986;46:6387–92.
10. Zhang JA, Xuan T, Parmar M, Ma L, Ugwu S, Ali S, Ahmad I. Development and characterization of a novel liposome-based formulation of SN-38. Int J Pharm 2004;270:93–107.
11. Kraut EH, Fishman MN, LoRusso PM, Gorden MS, Rubin EH, Haas A, Fetterly GJ, Cullinan P, Dul JL, Steinberg JL. Final result of a phase I study of liposome encapsulated SN-38 (LE-SN38): safety, pharmacogenomics, pharmacokinetics, and tumor response [abstract 2017]. Proc Am Soc Clin Oncol 2005;23:139S.
12. Koizumi F, Kitagawa M, Negishi T, Onda T, Matsumoto S, Hamaguchi T, Matsumura Y. Novel SN-38-incorporating polymeric micelles, NK012, eradicate vascular endothelial growth factor-secreting bulky tumors. Cancer Res 2006;66:10048–56.
13. Chou TC, Talalay P. Quantitative analysis of dose-effect relationships: the combined effects of multiple drugs or enzyme inhibitors. Adv Enzyme Regul 1984;22:27–55.
14. Azrak RG, Cao S, Slocum HK, Toth K, Durrani FA, Yin MB, Pendyala L, Zhang W, McLeod HL, Rustum YM. Therapeutic synergy between irinotecan and 5-fluorouracil against human tumor xenografts. Clin Cancer Res 2004;10:1121–9.
15. Jain RK. Barriers to drug delivery in solid tumors. Sci Am 1994; 271:58–65.
16. Savic R, Luo L, Eisenberg A, Maysinger D. Micellar nanocontainers distribute to defined cytoplasmic organelles. Science 2003;300:615–18.
17. Kawato Y, Aonuma M, Hirota Y, Kuga H, Sato K. Intracellular roles of SN-38, a metabolite of the camptothecin derivative CPT-11, in the antitumor effect of CPT-11. Cancer Res 1991;51:4187–91.
18. Slater R, Radstone D, Matthews L, McDaid J, Majeed A. Hepatic resection for colorectal liver metastasis after downstaging with irinotecan improves survival. Proc Am Soc Clin Oncol 2003;22(abstract 1287).
19. Araki E, Ishikawa M, Iigo M, Koide T, Itabashi M, Hoshi A. Relationship between development of diarrhea and the concentration of SN-38, an active metabolite of CPT-11, in the intestine and the blood plasma of athymic mice following intraperitoneal administration of CPT-11. Jpn J Cancer Res 1993;84:697–702.
20. Atsumi R, Suzuki W, Hakusui H. Identification of the metabolites of irinotecan, a new derivative of camptothecin, in rat bile and its biliary excretion. Xenobiotica 1991;21:1159–69.
21. Onda T, Nakamura I, Seno C, Matsumoto S, Kitagawa M, Okamoto K, Nishikawa K, Suzuki M. Superior antitumor activity of NK012, 7-ethyl-10-hydroxycamptoyhecin-incorporating micellar nanoparticle, to irrinotecan. Proc Am Assoc Cancer Res 2006;47:720s(abstract 3062).
22. Tournigand C, Andre T, Achille E, Lledo G, Flesh M, Mery-Mignard D, Quinaux E, Couteau C, Buyse M, Ganem G, Landi B, Colin P, et al. FOLFIRI followed by FOLFOX6 or the reverse sequence in advanced colorectal cancer: a randomized GERCOR study. J Clin Oncol 2004;22:229–37.
23. Colucci G, Gebbia V, Paoletti G, Giuliani F, Caruso M, Gebbia N, Carteni G, Agostara B, Pezzella G, Manzione L, Borsellino N, Misino A, et al. Phase III randomized trial of FOLFIRI versus FOLFOX4 in the treatment of advanced colorectal cancer: a multicenter study of the Gruppo Oncologico Dell'Italia Meridionale. J Clin Oncol 2005; 23:4866–75.

Expression profiling of fecal colonocytes for RNA-based screening of colorectal cancer

SATOSHI YAJIMA[1,2], MIE ISHII[3], HISAYUKI MATSUSHITA[4], KAZUHIKO AOYAGI[1], KAZUHIKO YOSHIMATSU[5], HIRONORI KANEKO[2], NOBUKO YAMAMOTO[3], TATSUO TERAMOTO[2], TERUHIKO YOSHIDA[1], YASUHIRO MATSUMURA[4] and HIROKI SASAKI[1]

[1]Genetics Division, National Cancer Center Research Institute, Tsukiji 5-1-1, Chuo-ku, Tokyo 104-0045; [2]Division of General and Gastroenterological Surgery (Omori), Department of Surgery, School of Medicine, Faculty of Medicine, Toho University, Omori Nishi 6-11-1, Ohta-ku, Tokyo 143-8541; [3]Medical Engineering Development Center, Canon Inc., Shimomaruko 3-30-2, Ohta-ku, Tokyo 146-8501; [4]Investigate Treatment Division, Research Center for Innovative Oncology, National Cancer Center Hospital East, Kashiwanoha 6-5-1, Kashiwa, Chiba 277-8577; [5]Medical Center East, Tokyo Women's Medical University, School of Medicine, Nishiogu 2-1-10, Arakawa-ku, Tokyo 116-8567, Japan

Received May 21, 2007; Accepted July 18, 2007

Abstract. The early detection of colorectal cancer originating from any part of the colorectum is desirable because this cancer can be cured surgically if diagnosed early. We searched for marker genes for a fecal RNA-based colorectal cancer screening method by comparison of genome-wide expression profiles among cancerous and non-cancerous tissues, and healthy volunteer- and cancer patient-derived colonocytes from the feces, and the peripheral blood. Of 14,564 genes, only 3 (PAP, REG1A, and DPEP1) were selectable as final candidates which were expressed frequently at any stage of this cancer and were suppressed in non-cancerous tissues and also in the peripheral blood and colonocytes of healthy volunteers. Next, we directly compared fecal RNA-expression profiles between colorectal cancer patients and healthy volunteers, and found that most of the genes (92%) expressed in the colonocytes of the cancer patients were not expressed in those of the healthy volunteers. Six genes (SEPP1, RPL27A, ATP1B1, EEF1A1, SFN, and RPS11) selected randomly from 85 cancer patient-derived colonocyte-specific genes were evaluated. In total, reverse transcription-polymerase chain reaction or focused microarray of all those 9 genes detected 18 (78%) of 23 curable colorectal cancers (Dukes stages A-C), 9 or 10 (64% or 71%) of 14 early cancers with no lymph node metastasis (Dukes stage A or B) and 4 (80%) of 5 right-sided cancers. Our extensive gene list provides other markers for fecal RNA-based colorectal cancer screening.

Correspondence to: Dr Hiroki Sasaki, Genetics Division, National Cancer Center Research Institute, Tsukiji 5-1-1, Chuo-ku, Tokyo 104-0045, Japan
E-mail: hksasaki@gan2.res.ncc.go.jp

Key words: expression profiling, colonocyte, colorectal cancer screening, microarray

Introduction

Colorectal cancer is a common malignancy which is curable by surgical resection if diagnosed at a sufficiently early stage (stage I/Dukes stage A or stage II/Dukes stage B). Five-year survival rates on surgical resection, for example, at Dukes stage A, Dukes stage B and stage III/Dukes stage C are 95%, 80% and 50-60%, respectively. For stage IV/Dukes stage D, curative resection is impossible. Therefore, early detection of this cancer originating from any part of the colorectum is desired. For mass cancer screenings, a simple, economic, and noninvasive method of cancer detection is required. The Hemoccult test is currently used in many countries for this purpose (1-5). However, this test is nonspecific and is not sufficiently sensitive to detect early-stage cancer, although a higher sensitivity has been reported for the advanced stage (6).

For fecal DNA-based colorectal cancer screening, in 1992, Sidransky first reported Ras oncogene mutations in the fecal DNA of patients with curable colorectal cancer (7). To date, many screening methods based on mutated DNA detection in the feces have been reported (8-19). These methods, however, are time-consuming and are not sufficiently sensitive. The major reason for this inaccuracy is the fact that fecal DNAs are derived from an enormous number and variety of bacteria and normal living cells including normal colorectal mucus cells, lymphocytes, red blood cells and anal squamous cells. Immunocytochemical analysis provides a simple method; however, this method is insensitive because only the surface portion of the feces can be assayed. On the other hand, Tarin and colleagues first reported that cancer-specific CD44 splicing variants are useful for fecal RNA-based colorectal cancer screening (20,21). By the use of the repetition of the Percoll centrifugation method for isolating the colonocytes from feces, we have also demonstrated that unusual CD44 variants could be targets for cancer-detection using feces (22). However, the method is found to distort the morphology of

colonocytes and to have a low retrieval rate. Accordingly, the sensitivity of this mRNA-based method also appears to be insensitive.

In any method for colorectal cancer detection using feces, an effective method which allows the simple isolation of the colonocytes from not only the surface but also the central portion of the feces while maintaining the initial morphology is needed. Recently, we successfully developed a new, very effective method that is based on the filtration of the homogenates of feces and magnetic cell sorting (MACS) with an epithelial cell-specific antibody, which we here abbreviated to FMCI (filtration and MACS-based colonocyte isolation) (23). It has been shown that this method can provide a high quality of colonocyte DNA or RNA for molecular biological analysis and also provide the colonocyte with its original morphology for cytology. Considering the advantage in the use of FMCI, we here report expression profiling of colonocytes for fecal RNA-based detection of curable colorectal cancer and a sensitive focused microarray assay that uses multiple marker genes for detecting minimal cancer cells in the feces of patients with colorectal cancer.

Materials and methods

Clinical materials. This study protocol was reviewed and approved by the Institutional Review Board of the National Cancer Center, Tokyo. Written informed consent was obtained from all the patients and healthy volunteers. Before surgical resection, stool samples were obtained from 23 patients with colorectal cancer (Dukes stages A-C), for which curable resection is possible, and from 15 healthy volunteers a few weeks after they had undergone a total colonoscopy. Naturally evacuated feces from subjects who had not taken laxatives were used as stool samples. Each patient was instructed to evacuate into a polystyrene disposable tray (AS one, Osaka, Japan) measuring 5x10 cm in size. Preparation of the stool samples for examination was conducted within 1-6 h after the evacuation. Tissue samples were obtained from the surgically resected specimens of colorectal cancer patients, and were snap frozen in liquid nitrogen and stored at -80°C until use. RNA of the tissues was extracted by using an Isogen kit (Nippon Gene, Toyama, Japan). The peripheral blood samples of 58 healthy volunteers and their RNA were prepared as in our previous report (24).

Isolation of exfoliated cells from feces. The procedure is detailed in our previous report (23). In brief, approximately 5-10 g of feces was used to isolate exfoliated cells. Feces were collected in Stomacher Lab Blender bags (Seward, Thetford, UK). The stool samples were homogenized with a buffer (200 ml) consisting of Hank's solution, 25 mM Hepes (pH 7.35), and 10% fetal bovine serum at 200 rpm for 1 min using a Stomacher (Seward). The homogenates were then filtered through a nylon filter (pore size, 512 μm), followed by division into 5 portions (40 ml each). Subsequently, 40 μl of magnetic beads coated with a mouse IgG1 monoclonal antibody (mAb Ber-EP4) specific for the glycopolypeptide membrane antigen Ep-CAM, which is expressed on most normal and neoplastic human epithelial cells (Dynal, Oslo, Norway), was added to each portion, and the mixtures were incubated for 30 min under gentle rolling in a mixer at room temperature. After 15-min shaking, the colonocytes were recovered from 5 tubes. The colonocytes from a single tube were stored at -80°C for RNA extraction. The colonocyte RNA was extracted by using an Isogen kit (Nippon Gene, Toyama, Japan).

Microarray analysis. We used human U133A Gene Chip (Affymetrix, Santa Clara, CA) for genome-wide expression profiling of mRNAs corresponding to 14,564 genes, 18,445 transcripts including splicing variants, and 22,215 probe sets. The procedures were conducted according to the supplier's protocols. Briefly, 10 μg of fragmented cRNA was hybridized to the microarrays in 200 μl of a hybridization cocktail at 45°C for 16 h in a rotisserie oven set at 60 rpm. The arrays were then washed with a nonstringent wash buffer (6X SSPE) at 25°C, followed by a stringent wash buffer [100 mM MES (pH 6.7), 0.1 M NaCl, and 0.01% Tween-20] at 50°C, stained with streptavidin phycoerythrin (Invitrogen, Carlsbad, CA), washed again with 6X SSPE, stained with biotinylated anti-streptavidin IgG, followed by a second staining with streptavidin phycoerythrin and a third wash with 6X SSPE. The arrays were scanned using a GeneArray scanner (Affymetrix) at 3-μm resolution, and the expression value (average difference: AD) of each gene was calculated using GeneChip Analysis Suite version 5.0 software (Affymetrix). The mean of AD values in each experiment was 1000 to reliably compare variable multiple arrays.

Reverse transcription-polymerase chain reaction (RT-PCR). RT-PCR on colonocyte RNA was carried out using primer sets designed for detecting the 3' side of cDNA of each gene. Primers were 5'-ACCAGTGTGAGGACTCACCC-3' and 5'-TGCTCTTTAAAGCCTTAGGCC-3' for PAP; 5'-AGCAATTACAACGGAGTCAA-3' and 5'-TCCAAAGACTGGGGTAGGT-3' for REGIA; 5'-TCTCTCCTGTGAAACCTGGG-3' and 5'-AAGGGGTGTTGCTTTTATTGC-3' for DPEP1; 5'-ATTAGCAGTTTAGAATGGAGG-3' and 5'-CTGTATCCAATTCTGTACTGC-3' for SEPP1; 5'-TGGGCTGCCAACATGCCATC-3' and 5'-TGTAGTAGCCCGATCGCACC-3' for RPL27A; 5'-GGCAAGCGAGATGAAGATAAGG-3' and 5'-AGGTCCCATACGTATGACAG-3' for ATP1B1; 5'-AGACTATCCACCTTTGGGTCG-3' and 5'-GATGCATTGTTATCATTAACCAGTC-3' for EEF1A; 5'-TTGAGCGCACCTAACCACTGGT-3' and 5'-GAGAGGAAACATGGTCACACCCA-3' for SFN, and 5'-ACATTCAGACTGAGCGTGCCTA-3' and 5'-GATCTGGACGTCCCTGAAGCA-3' for RPS11. PCR was performed under conditions of 30-35 cycles of 3 steps of temperature, 95°C for 1 min, 55°C for 1 min, and 72°C for 1 min, using the AccuPrime TaqDNA polymerase system (Invitrogen).

Marker gene detection using focused microarray. A focused microarray was constructed by fixing 50-60 mer of oligonucleotide probes on a slide glass using our previously developed Bubble Jet Technology (25). The microarray contained a single spot for each sequence of 9 marker genes (PAP, REG1A, DPEP1, SEPP1, RPL27A, ATP1B1, EEF1A1, SFN, and RPS11) and a control artificial DNA sequence. Each probe sequence used for the microarray is listed in Table I.

Table I. Sequences of primers and probes for focused microarray analysis.

Gene	Forward primers Reverse primers	Probes
PAP	GAGAAGCACAGCATTTCTGAG TGCTCTTTAAAGCCTTAGGCC	TTCCCCCAACCTGACCACCTCATTCTTATCTTTCTTCTGT TTCTTCCTCCCCGCTGTCAT
REG1A	AATCCTGGCTACTGTGTGAG TCCAAAGACTGGGGTAGGT	GACCATCTCTCCAACTCAACTCAACCTGGACACTCTCTT CTCTGCTGAGTTTGCCTTGTT
DPEP1	ACCCATTACGGCTACTCCTC AAGGGGTGTTGCTTTTATTGC	CAGATGCCAGGAGCCCTGCTGCCCACATGCAAGGACCA GCATCTCCTGAGAG
SEPP1	AATTAGCAGTTTAGAATGGAGG CTGTATCCAATTCTGTACTGC	CCATAGTCAATGATGGTTTAATAGGTAAACCAAACCCTA TAAACCTGACCTCCTTTATGG
RPL27A	TGGGCTGCCAACATGCCATC TGTAGTAGCCCGATCGCACC	CCAACTGTCAACCTTGACAAATTGTGGACTTTGGTCAGT GAACAGACACGGGTGAATGCT
ATP1B1	GGCAAGCGAGATGAAGATAAGG AGGTCCCATACGTATGACAG	GAGTGTAAGGCGTACGGTGAGAACATTGGGTACAGTGA GAAAGACCGTTTTCAGGGACGT
EEF1A1	AGACTATCCACCTTTGGGTCG GATGCATTGTTATCATTAACCAGTC	CCACCCCACTCTTAATCAGTGGTGGAAGAACGGTCTCAG AACTGTTTGTTTCAATTGGCC
SFN	TTGAGCGCACCTAACCACTGGT GAGAGGAAACATGGTCACACCCA	CTCTGATCGTAGGAATTGAGGAGTGTCCCGCCTTGTGGC TGAGAACTGGACAGTGG
RPS11	ACATTCAGACTGAGCGTGCCTA GATCTGGACGTCCCTGAAGCA	TCATCCGCCGAGACTATCTGCACTACATCCGCAAGTACA ACCGCTTCGAGAAGCG

Focused microarray analysis consists of 3 steps: i) Cy3-dUTP labeling by multiplex-RT-PCR; ii) hybridization Cy3-labeled cDNA to microarray, and iii) fluorescence scanning (Fig. 3). Using 0.5 to 1 μg of total RNA prepared from colonocytes, reverse transcription was performed with Superscript II (Invitrogen) with T7-oligo dT 24 primer in a total volume of 20 μl according to the manufacturer's protocol. To obtain 5-10 μg of cRNA, T7 transcription was performed. Using 5-10 μg of the cRNA, reverse transcription was performed with Superscript II with random hexamer in a total volume of 20 μl. Multiplex-RT-PCR was performed in two tubes at different PCR cycles: 35 cycles for PAP, REG1A and DPEP1, and 25 cycles for SEPP1, RPL27A, ATP1B1, EEF1A1, SFN, and RPS11. PCR primer sequences are also listed in supplementary Table II. Twenty-five μl of the PCR solution in each tube consisted of 1 μl of template cDNA, primers (6.25 pmol each), 50 μM Cy3-dUTP, 2.5 μl of AccuPrime 10X buffer1 (2 mM dNTP, 15 mM $MgCl_2$) and 1.0 μl of AccuPrime Taq polymerase (Invitrogen). A thermal cycler was set with initial heating at 95°C for 5 min followed by an amplification cycle heated at 95°C for 30 sec, 58°C for 30 sec and 72°C for 40 sec, followed by heating at 72°C for 10 min. The two PCR solutions were mixed and purified with a QIAquick PCR purification kit (Qiagen, Tokyo, Japan). The entire Cy3-labeled cDNA solution (50 μl) was mixed in 120 μl of a hybridization cocktail (6X SSPE containing 900 mM NaCl, 60 mM NaH_2PO_4, and H_2O, and 6 mM EDTA, pH 7.4/ 10% formamide/0.05% SDS) including 0.1 nM Cy3-labeled oligonucleotide which hybridizes the control artificial DNA sequence. By using a hybridization apparatus, HybStation (Genomic Solutions, Ann Arbor, MI), an array was pre-heated to 65°C for 3 min, filled with the hybridization cocktail, and incubated at 92°C for 2 min and then at 55°C for 4 h. Subsequently, the array was washed with 2X SSC, 0.1% SDS at 25°C and then with 2X SSC at 20°C, and rinsed with 0.1X SSC in accordance with a conventional manual, and finally dried by a spin drier. The array was scanned by an apparatus for DNA microarrays, Genepix 4000B (Axon Instruments, Union City, CA) and the fluorescence intensity from each probe spot was obtained after subtracting the background level. This focused microarray assay belongs in a negative or positive assay. However, it is required for determining the cutoff values. In this study, the maximum value of each gene plus 2- or 3-times standard deviation in 7 healthy volunteers was used as the cutoff-value.

Results

Marker gene selection through genome-wide expression profiles of cancer tissues, non-cancerous tissues, and the peripheral blood. In the feces of colorectal cancer patients, living cells other than bacteria include a small amount of cancer cells and normal colorectal mucus cells, lymphocytes, red blood cells and anal squamous cells. It is noted that the content of lymphocytes and red blood cells is increased in the feces of people with hemorrhoids. Therefore, genes that are expressed in almost all cases of early and advanced colorectal cancer and that are not expressed in normal colorectal mucosas,

Table II. Eighty-five genes expressed in the cancer patient-derived colonocytes but not in the healthy volunteer-derived colonocytes.

No.	Gene symbol	Gene title	Entrez gene ID	No expression in the PB
1	JUND	jun D proto-oncogene	3727	
2	TPT1	tumor protein, translationally-controlled 1	7178	*
3	RPL41	ribosomal protein L41	6171	*
4	RPS11	ribosomal protein S11	6205	*
5	RPS29	ribosomal protein S29	6235	*
6	RPL38	ribosomal protein L38	6169	*
7	SEPP1	selenoprotein P, plasma, 1	6414	*
8	RPL23	ribosomal protein L23	9349	*
9	B2M	ß-2-microglobulin	567	*
10	CFL1	cofilin 1 (non-muscle)	1072	*
11	RPL31	ribosomal protein L31	6160	*
12	RPS3A	ribosomal protein S3A	6189	
13	TMSB10	thymosin, ß 10	9168	*
14	RPL39	ribosomal protein L39	6170	*
15	HMGB1	high-mobility group box 1	3146	*
16	CEACAM6	carcinoembryonic antigen-related cell adhesion molecule 6 (non-specific cross reacting antigen)	4680	
17	ATP1B1	ATPase, Na^+/K^+ transporting, ß 1 polypeptide	481	*
18	RPS20	ribosomal protein S20	6224	*
19	ARF6	ADP-ribosylation factor 6	382	*
20	RPS21	ribosomal protein S21	6227	*
21	EIF5A	Eukaryotic translation initiation factor 5A	1984	*
22	RPL30	ribosomal protein L30	6156	*
23	EEF1A1	eukaryotic translation elongation factor 1 α 1	1915	*
24	RPL23A	ribosomal protein L23a	6147	*
25	LOC56902	putatative 28 kDa protein	56902	
26	RPL27	ribosomal protein L27	6155	*
27	SFN	stratifin	2810	*
28	CEACAM5	carcinoembryonic antigen-related cell adhesion molecule 5	1048	*
29	RPS24	ribosomal protein S24 /// ribosomal protein S24	6229	*
30	MARCKS	Myristoylated alanine-rich protein kinase C substrate	4082	*
31	PDE4C	phosphodiesterase 4C, cAMP-specific (phosphodiesterase E1 dunce homolog, *Drosophila*)	5143	
32	LOC651423	similar to mitogen-activated protein kinase kinase 3 isoform A	651423	
33	RPS10	ribosomal protein S10	6204	
34	CEP27	centrosomal protein 27 kDa	55142	
35	IL1RN	interleukin 1 receptor antagonist	3557	*
36	SLC35E1	solute carrier family 35, member E1	79939	
37	RPS27	ribosomal protein S27 (metallopanstimulin 1)	6232	*
38	RPS19	ribosomal protein S19	6223	*
39	RPS16	ribosomal protein S16	6217	*
40	MORF4L2	mortality factor 4 like 2	9643	*
41	RPL22	ribosomal protein L22	6146	*
42	RPS2	ribosomal protein S2	6187	*
43	RPLP2	ribosomal protein, large, P2	6181	*
44	RPL7A	ribosomal protein L7a	6130	
45	RPL7	ribosomal protein L7	6129	
46	RPS18	ribosomal protein S18	6222	*
47	HNRPH1	Heterogeneous nuclear ribonucleoprotein H1 (H)	3187	*
48	ZNF160	zinc finger protein 160	90338	

Table II. Continued.

No.	Gene symbol	Gene title	Entrez gene ID	No expression in the PB
49	RPS25	ribosomal protein S25	6230	*
50	PGF	Placental growth factor, vascular endothelial growth factor-related protein	5228	
51	SPG21	spastic paraplegia 21 (autosomal recessive, Mast syndrome)	51324	
52	RPL9	ribosomal protein L9	6133	*
53	PLEKHA5	Pleckstrin homology domain containing, family A member 5	54477	
54	PRR11	proline rich 11	55771	
55	CTNNB1	catenin (cadherin-associated protein), ß 1, 88 kDa	1499	*
56	NFKBIA	nuclear factor of κ light polypeptide gene enhancer in B-cells inhibitor, α	4792	*
57	GTSE1	G-2 and S-phase expressed 1	51512	
58	ATP8B1	ATPase, Class I, type 8B, member 1	5205	
59	TMED2	transmembrane emp24 domain trafficking protein 2	10959	*
60	RPS4X	ribosomal protein S4, X-linked	6191	
61	MUC3B	mucin 3B, cell surface associated	57876	
62	TTLL12	tubulin tyrosine ligase-like family, member 12	23170	
63	FTL	ferritin, light polypeptide	2512	*
64	TSPAN13	Tetraspanin 13	27075	*
65	PTP4A2	protein tyrosine phosphatase type IVA, member 2	8073	*
66	EGLN3	egl nine homolog 3 (C. elegans)	112399	*
67	ROCK2	Rho-associated, coiled-coil containing protein kinase 2	9475	
68	NDRG1	N-myc downstream regulated gene 1	10397	*
69	GTPBP1	GTP binding protein 1	9567	*
70	CAPZA1	capping protein (actin filament) muscle Z-line, α 1	829	*
71	RPL13	ribosomal protein L13	6137	*
72	CIDEC	cell death-inducing DFFA-like effector c	63924	*
73	SIRT3	sirtuin (silent mating type information regulation 2 homolog) 3 (S. cerevisiae)	23410	
74	LAPTM4A	lysosomal-associated protein transmembrane 4 α	9741	*
75	NOS1	nitric oxide synthase 1 (neuronal)	4842	*
76	COQ10B	coenzyme Q10 homolog B (S. cerevisiae)	80219	*
77	SAT	spermidine/spermine N1-acetyltransferase	6303	*
78	C1orf107	chromosome 1 open reading frame 107	27042	
79	TXN	thioredoxin	7295	*
80	SLC7A1	solute carrier family 7 (cationic amino acid transporter, y^+ system), member 1	6541	
81	SLC1A7	solute carrier family 1 (glutamate transporter), member 7	6512	
82	VIL2	villin 2 (ezrin)	7430	*
83	NTRK2	neurotrophic tyrosine kinase, receptor, type 2	4915	
84	GSTA1	Glutathione S-transferase A1	2938	
85	PTP4A3	protein tyrosine phosphatase type IVA, member 3	11156	

(*) Genes that were expressed in the cancer patient-derived colonocytes but not in either the healthy volunteer-derived colonocytes or the peripheral blood (PB) mixture.

peripheral blood, and squamous cells are potentially good markers for the screening of colorectal cancer from the feces. To identify effective genes for fecal RNA-based screening, we first compared 10 gene expression profiles of 6 early colorectal cancer tissues (2 Dukes stage A and 4 Dukes stage B cases), 3 advanced cancer RNA mixtures (6, 6, and 7 Dukes stage C or D cases), and a normal colorectal mucosa RNA mixture (6 cases). Of 14,564 genes, 2,926 were identified as genes which were not detected in the normal mucosa but detected in at least one of the above 9 cancer samples. Among these 2,926 cancer-specific genes, 205 genes, which were expressed in all of the 3 advanced cancer mixtures, were identified; however, only 3 genes were found to be expressed in all of the 6 early cancers. The cause of these results may

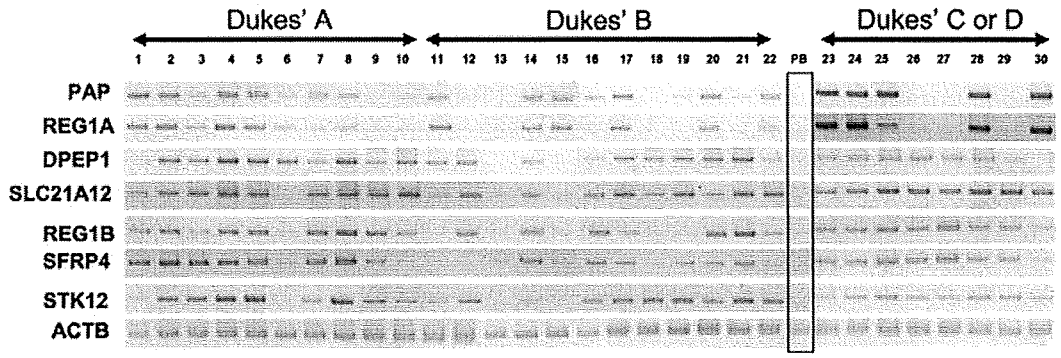

Figure 1. Results of RT-PCR of 7 genes (PAP, REG1A, DPEEP1, SLC21A12, REG1B, SFRP4, and STK12) selected by microarray analysis on 30 colorectal cancer tissues and on a peripheral blood mixture (PB). By microarray analyses, we first identified 15 genes which were expressed not in the normal colorectal mucosa mixture or in a peripheral blood mixture but in more than 4 of 6 early cancers (Dukes stage A or B) and in all of 3 advanced cancer mixtures (Dukes stage C or D). Next, we examined the frequency of the expression of these 15 genes in 30 colorectal cancer tissues (10 Dukes stage A, 12 Dukes stage B, and 8 Dukes stage C or D cancers), and selected, by RT-PCR, 7 genes (PAP, REG1A, DPEP1, SLC21A12, REG1B, SFRP4, and STK12) as the frequently expressed genes at any stage of colorectal cancer.

be that the expression profile of early cancer varies from case to case. Of 14,564 genes, we were able to select 65 genes which were expressed not in the normal colorectal mucosa mixture but in more than 4 of the 6 early cancers and in all of the 3 advanced cancer mixtures.

Considering bleeding by nonmalignant diseases such as hemorrhoids, which often give false positives in fecal colorectal cancer screening, we selected 15 genes from the 65 genes, because the expression of all the other 50 genes was detectable in a peripheral blood mixture of 58 healthy volunteers when a highly sensitive nested RT-PCR analysis with outer and inner primer sets was performed (data not shown). Next, we examined the frequency of the expression of these 15 genes in 30 colorectal cancer tissues (10 Dukes stage A, 12 Dukes stage B, and 8 Dukes stage C or D cancers), and selected, by RT-PCR, 7 genes (PAP, REG1A, DPEP1, SLC21A12, REG1B, SFRP4, and STK12) as the frequently expressed genes at any stage of colorectal cancer (Fig. 1). By RT-PCR, we lastly checked the expression of these 7 genes in RNA samples of the colonocytes of 15 healthy volunteers, which were isolated from the feces by FMCI (23). No mRNA expression of 3 genes (PAP, REG1A, and DPEP1) was detected in the colonocyte samples of all the 15 healthy volunteers; however, the other 4 genes (SLC21A12, REG1B, SFRP4, and STK12) were found to be expressed in some samples (data not shown). This fact may be due to the contamination of anal squamous cells, which were dissociated from the anus and survived in the feces, because our gene selection process can minimize the effect on the contamination of lymphocytes, red blood cells and dissociated normal colorectal epithelium. Under the above criteria, only 3 genes were selected as the final candidates for the fecal RNA-based early detection of colorectal cancer.

Marker gene selection by comparison of expression profiles between healthy volunteer- and cancer patient-derived colonocytes from the feces. Next, we obtained and compared 5 gene expression profiles of 4 colonocyte RNA samples (CF15, CF17, CF18, and CF25), which were isolated from the feces of 4 colorectal cancer patients by FMCI, and a colonocyte RNA mixture (HVF) of 7 healthy volunteers. Of 14,564 genes, the number of detectable genes in 5 colonocyte samples, CF15, CF17, CF18, CF25, and HVF is 768, 603, 772, 459, and 326, respectively. The number of detectable genes in the colonocyte is approximately 6.5% of that (11,343) in the colorectal cancer tissue. The major reason seems to be that most colonocytes are not in the cell division cycle but are resting, because the detectable gene number (1,535) in the peripheral blood composing such resting cells was also small. Unexpectedly, 716 (93%), 553 (92%), 712 (92%), and 424 (92%) of the above detectable genes (768, 603, 772, and 459) in the the colonocytes of the cancer patients were not expressed in those of the healthy volunteers. The huge difference of the colonocyte expression profiles between the colorectal cancer patients and the healthy volunteers might lead to success in gene selection for fecal RNA-based early detection of colorectal cancer. Eighty-five genes, whose expression was found in 3 or 4 of the 4 colorectal cancer patient samples (CF15, CF17, CF18, and CF25) but not in the HVF, were identified (Table II). Of these 85 genes, 29 (34%) were found to encode ribosomal proteins (RPLs or RPSs). In the course of a series of studies, it is predicted that normal mucous cells will die and be exfoliated during turnover and that the colorectal cancer cells will survive for a long time in the isolation processes as well as in the feces (22,23). Therefore, protein synthesis in the cells would be maintained actively for cancer cell survival under these conditions. The FMCI can minimize the contamination of both lymphocytes and red blood cells because the FMCI contains the enrichment process of epithelial cells such as colorectal cancer cells, the contaminated anal squamous cells, and a few living cells dissociated from the normal colorectal mucosa by MACS (23). Therefore, expression status in the peripheral blood is not needed for the gene selection process for fecal RNA-based screening; all of the 85 genes are expected to be good markers if the colonocytes are isolated by FMCI.

RT-PCR and focused microarray analyses of 9 selected genes in 30 colonocyte RNA samples. Next, we performed RT-PCR of the first 3 identified genes (PAP, REG1A, and DPEP1) in the colonocyte RNA samples which were prepared from 23 curable colorectal cancer patients (Dukes stages A-C) and 7 healthy volunteers. The 23 colorectal cancer patients were 8